Title

A new centrosomal protein regulates neurogenesis by microtubule organization

Authors:

Germán Camargo Ortega[1-3†], Sven Falk[1,2†], Pia A. Johansson[1,2†], Elise Peyre[4], Sanjeeb Kumar Sahu[5], Loïc Broic[4], Camino De Juan Romero[6], Kalina Draganova[1,2], Stanislav Vinopal[7], Kaviya Chinnappa[1‡], Anna Gavranovic[1], Tugay Karakaya[1], Juliane Merl-Pham[8], Arie Geerlof[9], Regina Feederle[10,11], Wei Shao[12,13], Song-Hai Shi[12,13], Stefanie M. Hauck[8], Frank Bradke[7], Victor Borrell[6], Vijay K. Tiwari[§], Wieland B. Huttner[14], Michaela Wilsch-Bräuninger[14], Laurent Nguyen[4] and Magdalena Götz[1,2,11*]

Affiliations:

1. Institute of Stem Cell Research, Helmholtz Center Munich, German Research Center for Environmental Health, Munich, Germany.
2. Physiological Genomics, Biomedical Center, Ludwig-Maximilian University Munich, Germany.
3. Graduate School of Systemic Neurosciences, Biocenter, Ludwig-Maximilian University Munich, Germany.
4. GIGA-Neurosciences, Molecular regulation of neurogenesis, University of Liège, Belgium
5. Institute of Molecular Biology (IMB), Mainz, Germany.
6. Instituto de Neurociencias, Consejo Superior de Investigaciones Científicas and Universidad Miguel Hernández, Sant Joan d'Alacant, Spain.
7. Laboratory for Axon Growth and Regeneration, German Center for Neurodegenerative Diseases (DZNE), Bonn, Germany.
8. Research Unit Protein Science, Helmholtz Centre Munich, German Research Center for Environmental Health, Munich, Germany.

9. Protein Expression and Purification Facility, Institute of Structural Biology, Helmholtz Center Munich, German Research Center for Environmental Health, Munich, Germany.
10. Institute for Diabetes and Obesity, Monoclonal Antibody Core Facility, Helmholtz Center Munich, German Research Center for Environmental Health, Munich, Germany.
11. SYNERGY, Excellence Cluster of Systems Neurology, Biomedical Center, Ludwig-Maximilian University Munich, Germany.
12. Developmental Biology Program, Sloan Kettering Institute, Memorial Sloan Kettering Cancer Center, New York, USA
13. BCMB Allied Graduate Program, Weill Cornell Medical College, New York, USA
14. Max Planck Institute of Molecular Cell Biology and Genetics, Dresden, Germany.

*Correspondence to: magdalena.goetz@helmholtz-muenchen.de
†These authors contributed equally
‡Current address: Instituto de Neurociencias, Consejo Superior de Investigaciones Científicas and Universidad Miguel Hernández, Sant Joan d'Alacant, Spain.
§Previous address: Institute of Molecular Biology (IMB), Mainz, Germany

Abstract

The expansion of brain size in species with a large and gyrified cerebral cortex is triggered by a relative enlargement of the subventricular zone (SVZ) during development. Here, we uncover the key role of the novel interphase centrosome protein Akna in this process and show that it localizes mainly at subdistal appendages of the mother centriole in subtypes of neural stem and progenitor cells. Akna is necessary and sufficient to organize microtubules (MT) at the centrosome and regulate their polymerization. These processes show an unprecedented role of MT dynamics controlled by Akna in regulating entry to, and exit from, the SVZ by controlling delamination from the neuroepithelial ventricular zone and retention

of cells in the SVZ. Importantly, Akna plays a similar role in mammary epithelial cells undergoing epithelial-to-mesenchymal transition (EMT), generalizing the importance of this new centrosomal protein in orchestrating MT polymerization to control cell delamination.

Main Text

Expansion of the SVZ is the developmental hallmark of enlarged and folded cerebral cortices, underpinning the importance of understanding the mechanisms that govern its formation. Epithelial-like neural stem cells (NSCs) divide in the ventricular zone (VZ), and mostly generate a new NSC and a committed progenitor cell at midneurogenesis. The latter delaminates and transforms into a basal progenitor (BP) which constitute the SVZ[1,2]. Keeping cells for a defined temporal window in the SVZ is essential to control further amplification and fate determination[3,4]. To identify novel regulators of these processes we compared the transcriptome of murine NSC sub-types that generate BPs from those that do not[5-7]. We report here a novel and unexpected regulator of BP generation and SVZ formation, called Akna. Our work uncovers the function of this mis-annotated protein at the centrosome and reveals interphase centrosomal microtubule organizing center (MTOC) activity as a novel mechanism regulating EMT-like delamination of cells from the VZ to enter the SVZ and their retention therein.

Akna is an integral component of the interphase centrosome

In murine cerebral cortex, Akna mRNA levels correlate with the time of SVZ generation (low at embryonic day 11 (E11), high at E14, low at E18) and NSCs isolated at the peak of SVZ generation have higher Akna levels when transitioning to BPs[6] (Extended Data Fig. 1a,b). We therefore chose Akna as a candidate regulator of SVZ and BP generation and generated several rat and mouse monoclonal antibodies against Akna, validated by means of RNA interference, to test this hypothesis further (Extended Data Fig. 1c-f, information about clones

used in Methods). Given the annotation of Akna as a transcription factor[8], we were surprised to find specific immunofluorescence (IF) signals at centrosomes (Fig. 1a and Extended Data Fig. 1f, g) in different cell types (B cells, cell lines, NSCs, cerebral cortex cells) of murine, ferret, primate and human origin (Extended data Figs. 1-4,7,9). This location was confirmed using BAC-transgenic cell lines with a c-terminal EGFP-tag (Extended Data Fig. 1h). Indeed, Akna lacks a nuclear localization signal and, in mice, the GRP core motif[9] of the AT hook domain required for RNA and DNA binding (see Extended Data Fig. 1i, j) and is not detectable in the nuclear fraction (Extended Data Fig. 1k), but rather in centrosome enriched fractions (Extended Data Fig. 1l).

Using immune electron microscopy (EM) to detect endogenous Akna in the mouse brain and STED nanoscopy in cultured NSCs we found that Akna largely localizes at the distal part of the subdistal appendages (SDAs) of the mother centriole (MC) in interphase, although a minor signal is also detected in the proximal ends (PEs) of both centrioles, (Extended Data Fig. 2a-c and Supplementary Movie 1). Importantly, the carboxyterminal part of Akna is necessary for its localization at the centrosome (a region omitted in its first description[8]), with all forms lacking these last 370 amino acids distributing within the cytoplasm (Extended Data Fig. 2d-k). The centrosomal localization of Akna is not MT- or cargo-motor dependent, since it remained at centrosomes upon treatment with: 1) the MT de-polymerization factor, nocodazole; 2) the MT stabilization factor, Taxol (not shown); 3) destabilization of the Dynein/Dynactin complex by p50/Dynamitin (Dcnt2) overexpression (Extended Data Fig. 2i-k). Akna is an integral SDA component as it was lost from the centrosome remnants in the cerebral cortex of Sas4/P53 double knock-out mice, that lack centrioles but retain pericentriolar material (containing pericentrin (Pcnt), Extended Data Fig. 2l) and it also disappeared from the centrosome upon deletion of the SDA protein Odf2 (Extended Data Fig. 2m, n).

During mitosis, Akna was no longer detectable at the centrosomes or spindle poles (Extended

Data Fig. 1h'', 3a), as is often the case for SDA-associated proteins.[10-12] Immunoblots of synchronized cells and live imaging of Akna-Kusabira-Orange (mKO2) fusion protein showed that Akna is not degraded during M-phase, but rather dissociates from the centrosome and reassembles there in late telophase and G1 (Extended Data Fig. 3b and Supplementary Movie 2). This process is regulated by phosphorylation as inhibition of phosphatases by okadaic acid (OA) led to the delocalization of Akna from the centrosome in primary cerebral cortex cells 3-4 hours after treatment (Extended Data Fig. 3c, d). Thus, Akna is a novel interphase centrosome protein raising the question about its role in development.

Akna regulates NSCs delamination and seeding of the SVZ

To understand Akna's function in the developing murine cerebral cortex, we first determined which cells have Akna positive (Akna+) centrosomes. Consistent with mRNA analysis, only a few centrosomes were very weakly Akna+ before (E9) and at the end of (E18) neurogenesis (Extended data Fig. 4a, b). Conversely, at E14, the peak of SVZ generation, Akna+ centrosomes were present and their number were highest in the SVZ (Fig. 1b, c; Extended data Fig. 4c), while almost no signal was observed in the layer of differentiating neurons, the cortical plate (CP). At the apical surface of the VZ, only a fraction of centrosomes (20% and 46% quantified by IF and EM respectively, Extended Data Fig. 4d, e) were Akna+. These NSCs with Akna+ centrosomes were Pax6+/Tbr2+ differentiating NSCs[13] as shown in both primary cultures (4 hours post isolation) and FACS-sorted Prominin1+ NSCs, in full agreement with Akna mRNA expression profile[13] (Extended Data Fig. 4f, g). Thus, Akna exhibits an unprecedented subtype-specificity for a centrosomal protein largely restricted to differentiating NSCs and BPs.

To functionally analyze the role of Akna in corticogenesis, we used shRNA mediated knock-down (KD) (see WB in Extended Data Fig. 1d) via *in utero* electroporation (IUE) at E13. In control conditions, large proportions of GFP+ cells had left the VZ and SVZ of the cerebral

cortex and were migrating into the CP two days after IUE (Fig. 2a). In contrast, under Akna KD conditions, GFP+ cells were mainly retained in the VZ and SVZ with very few migrating towards the CP (Fig. 2c and Supplementary Video 3). Notably, this phenotype was observed upon KD with 2 different shRNAs, and also occurred when p53-mediated cell death induced by Akna KD was blocked (Fig. 2b, c, Extended data Fig. 5). According to the positional changes upon Akna knock-down with more cells in the VZ, we also observed an increase in Pax6+/Tbr2- NSCs and decrease in Pax6-/Tbr2+ BPs (Fig. 2d). Thus, Akna loss-of-function impairs NSC delamination and subsequently blocks further lineage progression.

Conversely, Akna OE in E13 cortex induced delamination of NSCs from the VZ with most electroporated GFP+ cells being in the SVZ already 24 hours after IUE (Fig. 2e-g). Accordingly, Akna OE also induced higher percentages of Tbr2+ BPs and NeuN+ neurons, with a concomitant decrease in Pax6+ and Ki67+ cells, as compared to controls (Fig. 2h, i). Live imaging in cortical slices showed that this accelerated delamination occurred by retraction of the apical processes without undergoing cell division (28%, n=33 compared to 3%; n=165, in controls, Supplementary Video 4). Thus, the delamination induced by Akna OE does not require M-phase or the orientation of cell division when other centrosomal proteins act, but rather occurs in interphase, when endogenous levels of Akna are also at their peak. Akna gain-of-function thus induces precocious delamination and subsequently premature neuronal differentiation.

Akna affects microtubule organization in subtypes of neural progenitors

To determine how Akna mediates the effects described above, we first examined whether Akna OE also elicits cell fate changes *in vitro*. When Akna was overexpressed for 48 hours in dissociated E14 cortex primary cells no changes in the proportion of Pax6+, Tbr2+ or Ki67+ cells were observed (Fig. 2j). This suggests that the increased neuronal differentiation

observed upon Akna OE *in vivo* likely occurs due to re-localization to the SVZ niche (Fig. 2k).

We next asked how Akna could mediate the delamination of cells from the VZ. So far only mechanisms influencing the F-actin belt and the adherens junctions (AJs) between NSCs as well as primary cilium positioning have been implicated in retaining NSCs in the VZ[14-16]. Given the localization of Akna at the SDAs that anchor MTs, we suspected a different role of Akna and used nocodazole wash-out assays to monitor MT regrowth (Extended Data Fig. 6a) upon shRNA-mediated Akna knock-down (KD) in E14 primary cortical cells (Fig 3a). Interestingly, the proportion of cells exhibiting centrosomal MT regrowth was significantly reduced compared to control transfected cells with the remaining cells (which still showed centrosome-based nucleation) having an overall reduction in length of the MT fibers (Fig. 3a-c). Thus, lowering Akna protein levels dramatically reduces centrosomal interphase MTOC activity *in vitro*.

To determine whether Akna is also sufficient to organize MTs we transfected E14 primary cortical cells with Akna expressing plasmids and performed the nocodazole wash-out assay. Strikingly, MT-asters emanated from ectopic Akna protein foci (Fig. 3d and Extended Data Fig. 6b) that were also sufficient to recruit gamma-Tubulin Ring Complex (gTurC) components gamma-Tubulin (Tubg) and Tubgcp4 (Extended Data Fig. 6c). Neither the MT-minus end capping-protein - Camsap2 - nor the centrosomal protein - Pcnt - were enriched at Akna foci, ruling out unspecific binding of antibodies to Akna foci (Extended Data Fig. 6d). Thus, Akna is sufficient to recruit mainly gTuRC-capped MTs and proteins involved in MT organization at SDAs such as Mapre1/EB1, Dctn1/p150Glued and Odf2[17-20] (Extended Data Fig. 6e). Co-immunoprecipitation experiments proved association of Akna with EB1, Dctn1 and Odf2, but not with the gTuRC component Tubgcp2 (Extended Data Fig. 6f), suggesting Akna organizes MTs together with the above-mentioned proteins at SDAs while its interaction with gTuRC may be weaker or indirect. Thus, we identified here a novel regulator

of centrosomal MTOC activity selectively enriched in differentiating NSCs. This is intriguing as centrosomal MTOC activity regulated by Akna may counteract the often non-centrosomal MT anchoring in epithelial cells mediated by the Camsap-family of proteins[21] and thereby change the major mode of MT anchoring and polymerization in delaminating NSCs.

To directly observe such changes *in vivo*, we monitored growing MTs by live imaging in slice preparations using EB3-GFP after Akna IUE. Consistent with previous data[22], EB3-GFP comets preferentially moved basally into the radial glial process in control cells with an average angle of 78° relative to the apical surface (Fig. 3e, f). Upon Akna OE, we observed comets moving more obliquely (average angle 55°, Fig. 3e, g; Supplementary Videos 5, 6), indicating a change in the orientation of MT nucleation and repositioning of the MTOC to non-apical positions. Moreover, the speed of the EB3-GFP comets was significantly higher upon Akna OE, suggesting that MT polymerization speed is increased when Akna levels are high (Fig. 3h). On the contrary, upon lowering Akna levels with shRNA constructs harboring a EB3-neonGreen reporter, we observed a significant reduction in EB3 comet speed (Fig. 3i and Supplementary Videos 7,8). Together this indicates, in agreement with the above observations, that knocking down Akna decreases MT polymerization. Hence, Akna levels regulate MT nucleation and organization in the cell and influence MT polymerization both *in vitro* and *in vivo*. This suggests that Akna levels are critical to shift the balance of MTs anchored at non-centrosomal positions, such as in the basal process and at AJs in NSCs with epithelial hallmarks[2,23-25], to the centrosome which is also accompanied by faster MT polymerization. This in turn might be necessary for destabilization of AJs mediating the delamination observed *in vivo*.

Akna is required during EMT

As the delamination from the VZ is regulated by transcription factors also involved in EMT[26,27], we examined if the cell biological mechanisms of delamination mediated by Akna

may also be relevant in true epithelial cells undergoing EMT. Towards this aim, we monitored normal murine mammary gland epithelial cells (NMuMG) during EMT induced by Transforming growth factor beta-1 (TGF-beta-1)[28,29]. While epithelial NMuMG cells have low levels of Akna, it is up-regulated during EMT and localizes to the centrosome (Extended Data Fig. 7a-c). Since epithelial cells show largely non-centrosomal MT polymerization prior to EMT[21], we hypothesized that, in analogy to NSCs, Akna might redirect MTOC activity to the centrosome during EMT and thereby critically control EMT progression. To determine the role of Akna in EMT, we used siRNAs to reduce its levels (Extended Data Fig. 7d). While TGF-beta-1 mediated EMT induction in Akna knockdown conditions leads to a similar upregulation of core EMT transcription factors like Twist and Zeb1 and the mesenchymal target Fibronectin (data not shown), we observed the retention of the tight junction component ZO1 (Fig. 4a-c) and increased levels of ZO1 and the cadherin interactor p120 (Extended Data Fig. 7e, f). Moreover, the rearrangement of the actin cytoskeleton from the AJs to stress fibers, visualized by Phalloidin stainings was attenuated upon knock-down of Akna and still visible at many cell-cell contacts (Fig. 4a''-c'') and cells remained closer together (Extended data Fig. 7g-i). Thus, Akna plays a key role in disassembling junctional coupling during EMT. Taken together, these and the above data suggest that Akna up-regulation leads to the re-distribution of MTs anchored through p120 at the junctional complex[23] to a centrosome-based array, thereby facilitating the dissolution of cell-cell contacts that ultimately allows mesenchymal cell scattering. To determine whether Akna also contributes to dissolving junctional coupling in the developing cerebral cortex, we examined brains shortly after Akna OE (18h after IUE; Fig. 4d, e) prior to delamination of most cells (Fig. 2f, g). In agreement with the results obtained in mammary epithelial cells, Akna OE also reduced E-cadherin levels within electroporated areas in the cortical VZ (Fig. 4e). Thus, Akna controls previously unanticipated changes at the centrosome required for EMT and NSC to BP progression. This

provides new insights into how changing MT dynamics may contribute to remodeling of the junctional complexes allowing cells to delaminate from their epithelial neighbors.

Akna regulates retention of cells within the SVZ

Given Akna's function in regulating MTOC activity and MT polymerization, we next examined young neurons in the CP that lose Akna at the centrosomes (only 10% of centrosomes are Akna+; Extended data Fig. 4e). As expected, neurons isolated by FACS (PSA-NCAM+ cells) from E14 cerebral cortices showed much more non-centrosomal MT polymerization in nocodazole-based MT regrowth assays (Extended Data Fig. 8a, b; compare to NSCs), consistent with the decline of Akna in neurons and its role in mediating the centrosomal MTOC activity. To determine the function of Akna when cells progress from a multipolar state in the SVZ to a bipolar migratory phase entering the CP *in vivo*, we first expressed Akna cDNA under the late BP/neuron-specific Doublecortin (Dcx)-promoter (Extended Data Fig. 8c) at E13. When control cells were analyzed 5 days later most had progressed into the CP, while approx. 50% of the GFP+ Akna OE cells were retained below the CP (Fig. 5a-d). These were still able to differentiate into neurons and extend callosal projections (Extended Data Fig. 8d-f). Conversely, downregulating Akna in late BPs and young neurons by Dcx-promoter driven Akna miRNAs did not affect cells leaving the SVZ and reaching normal positions within the CP similar to controls (Extended Data Fig. 8g, h). Thus, increasing Akna levels prevents cells from moving into the CP indicating that physiologically occurring Akna downregulation (Fig. 1b; Extended Data Fig. 1a, 4a-f) is crucial in this transition.

To determine at which step Akna levels are critical in this transition from multipolar SVZ cells to bipolar neurons migrating into the CP[30], we performed live imaging in slices upon Akna OE or knock-down. Control and KD cells had similar migration speed (Fig. 5e), but KD cells transited even faster from the multipolar SVZ morphology to a bipolar migrating

neuronal morphology (Fig. 5f, g). In contrast, many Akna OE cells retained a multipolar morphology and migrated less (Fig. 5h,i and Supplementary Videos 9 and 10), demonstrating the key role of Akna not only in bringing cells into the SVZ, but also in retaining them there.

Akna levels affect SVZ formation in species with gyrified cortex

Retaining cells in the SVZ is particularly important in species with an expanded outer SVZ (oSVZ), such as ferrets and primates[31]. Indeed, Akna mRNA in ferret VZ peaks at the onset of oSVZ formation when most cells forming the oSVZ delaminate (Extended Data Fig. 9a) and differs in abundance at centrosomes in the oSVZ of future sulcus and gyrus regions (Extended Data Fig. 9b-f). Indeed, Akna is also enriched at centrosomes in primate oSVZ, but not detectable in the CP (Extended Data Fig. 9g, h). A feature that is fully consistent with its role in mediating entry and exit to and from the SVZ in mice. To corroborate this at the functional level in human cells, we first showed that AKNA is sufficient to organize MTs also in human induced pluripotent stem cell (iPSC)-derived NSCs (Extended Data Fig. 9i, i'). We next used AKNA OE (2 days) and KD (5 days) to test its function in human cerebral organoids grown for 7-8 weeks following the Lancaster protocols[32,33]. Importantly, AKNA OE also mediated delamination from the VZ in human cortex organoids (Extended data Fig. 9l-n) and its KD lead to a significant increase in retention of cells in the VZ (Extended data Fig. 9o). Thus, the conserved function of Akna in recruiting and retaining cells in the SVZ may allow dynamical change of SVZ size during evolution.

Discussion

Our work identified and characterized the function of a new component of the centrosome, the former mis-annotated AT-hook transcription factor Akna, and reveals hitherto unknown cell biological aspects controlling neurogenesis. We show that Akna confers centrosomal MTOC

activity during interphase specifically in subtypes of NSCs and progenitor cells. Akna is downregulated during neuronal differentiation concomitant with the change in MT organization in neurons, i.e. from primarily centrosome- to more non-centrosome-based organization. In neurons, MTs originate preferentially from other subcellular compartments such as the Golgi apparatus, the cell cortex or local pools of MTs[34], allowing the generation of axons and dendrites while still moving into and within the CP[35,36]. Indeed, reduction of Akna levels is a requirement for neurons to proceed into the CP as its OE under Dcx-promoter blocks this process. The molecular mechanisms of centrosome inactivation are not well understood. Previously, re-localization of some nucleating and anchoring factors such as Tubg, Cdk5rap2 (i.e. gTuRCs) and Ninein, as well as the down-regulation of Nedd1[35,37] have been implicated. Here, we propose that Akna is an important regulator of the loss of centrosomal MTOC activity in neurons[38]. Importantly, we demonstrate that this switch occurs at early stages of neuronal differentiation and is critical in regulating the exit from the SVZ.

Most strikingly, Akna also promotes entry into the SVZ as demonstrated by cells remaining in the VZ upon knock-down and their fast delamination in interphase upon overexpression in the VZ. *In vivo* live imaging upon Akna manipulation clearly demonstrated that it not only regulates centrosomal MTOC activity, but also affects MT polymerization. Thus, Akna affects at least two aspects of the delamination process. Firstly, the increase in MT polymerization as mediated by Akna in differentiating NSCs could weaken cellular junctions and hence promote the release of cells towards the SVZ. Indeed, MT polymerization per se decreases p120-mediated stability of cadherins in cell lines[39]. Moreover, members of the Camsap/Patronin protein family promote MT nucleation at cellular junctions or, together with Katanin, release centrosomal MTs[40] and tether them to the AJs[21]. This contributes, through interaction with p120, to AJ stability.[23,41] Importantly, if Camsaps are downregulated, centrosomal MT nucleation increases[40] and both cell adhesion and junctional organization is

distorted.[42] Our data thus supports a model in which Akna-mediated recruitment of MTs to the centrosome reduces MTs at the junctional complex, thereby destabilizing it. This is supported by the effects of Akna KD in mammary epithelial cells undergoing EMT impairing the complete detachment of cells and retention of junctional components. Secondly, positioning of the centrosome is affected by changes in MT organization upon Akna manipulation. This may help to polarize organelles towards the SVZ[43] when cells become multipolar and leave the VZ. Likewise, Akna levels need to be down-regulated when multipolar SVZ cells become bipolar again when moving to the CP[30]. Indeed, MT dynamics regulate cell polarity by influencing centrosome and Golgi apparatus repositioning in cell lines[44,45]. Moreover, EMT in many developing organs is accompanied by changing polarity and centrosome positioning[44]. As Akna loss and gain of function experiments show changes in the angle of MT polymerization after Akna OE and polarity defects in newborn neurons, we propose that Akna plays a key role in mediating the changes in polarization when bipolar RGCs transit to multipolar BPs (requiring high Akna levels) and when multipolar cells in the SVZ progress towards bipolar migrating neurons (requiring low Akna levels).

Thus, Akna is a novel centrosomal protein crucially involved in the regulation of cell delamination in the developing brain and other epithelial cells undergoing EMT, a wide-spread process in many developing tissues[44]. As neither Akna loss- nor gain-of-function have any apparent effect on cilia growth, maintenance or position in cortical progenitors neither *in vivo* nor *in vitro* (Extended Data Fig. 10), we conclude that Akna does not exert its effects via cilia-mediated mechanisms. Importantly, the Akna phenotype and functions outlined here differ from previously reported centrosome associated proteins in the developing cerebral cortex often regulating spindle formation and orientation[46-48]. Interestingly, knockdown of the SDA protein Ninein in NSCs has the opposite effect than Akna KD, namely triggering delamination[49], suggesting that Akna may counteract Ninein in a subtype-specific manner.

Most importantly, Akna is the first and only known centrosomal protein regulating entry to and exit from the SVZ thereby not only coordinating both of these processes, but also highlighting the importance in the balance of centrosomal versus acentrosomal MT recruitment in this crucial event during ontogeny and phylogeny of the brain.

References:

1 Konno, D. *et al.* Neuroepithelial progenitors undergo LGN-dependent planar divisions to maintain self-renewability during mammalian neurogenesis. *Nat Cell Biol* **10**, 93-101 (2008).

2 Taverna, E., Gotz, M. & Huttner, W. B. The cell biology of neurogenesis: toward an understanding of the development and evolution of the neocortex. *Annu Rev Cell Dev Biol* **30**, 465-502 (2014).

3 Martinez-Martinez, M. A. *et al.* A restricted period for formation of outer subventricular zone defined by Cdh1 and Trnp1 levels. *Nat Commun* **7**, 11812 (2016).

4 Fernandez, V., Llinares-Benadero, C. & Borrell, V. Cerebral cortex expansion and folding: what have we learned? *EMBO J* **35**, 1021-1044 (2016).

5 Pinto, L. *et al.* AP2gamma regulates basal progenitor fate in a region- and layer-specific manner in the developing cortex. *Nat Neurosci* **12**, 1229-1237 (2009).

6 Pinto, L. *et al.* Prospective isolation of functionally distinct radial glial subtypes--lineage and transcriptome analysis. *Mol Cell Neurosci* **38**, 15-42 (2008).

7 Stahl, R. *et al.* Trnp1 regulates expansion and folding of the mammalian cerebral cortex by control of radial glial fate. *Cell* **153**, 535-549 (2013).

8 Siddiqa, A. *et al.* Regulation of CD40 and CD40 ligand by the AT-hook transcription factor AKNA. *Nature* **410**, 383-387 (2001).

9 Filarsky, M. *et al.* The extended AT-hook is a novel RNA binding motif. *RNA Biol* **12**, 864-876 (2015).

10 Nigg, E. A. & Stearns, T. The centrosome cycle: Centriole biogenesis, duplication and inherent asymmetries. *Nat Cell Biol* **13**, 1154-1160 (2011).

11 Chretien, D., Buendia, B., Fuller, S. D. & Karsenti, E. Reconstruction of the centrosome cycle from cryoelectron micrographs. *J Struct Biol* **120**, 117-133 (1997).

12 Vorobjev, I. A. & Chentsov Yu, S. Centrioles in the cell cycle. I. Epithelial cells. *J Cell Biol* **93**, 938-949 (1982).

13 Aprea, J. *et al.* Transcriptome sequencing during mouse brain development identifies long non-coding RNAs functionally involved in neurogenic commitment. *EMBO J* **32**, 3145-3160 (2013).

14 Paridaen, J. T., Wilsch-Brauninger, M. & Huttner, W. B. Asymmetric inheritance of centrosome-associated primary cilium membrane directs ciliogenesis after cell division. *Cell* **155**, 333-344 (2013).

15 Schmid, M. T. *et al.* The role of alpha-E-catenin in cerebral cortex development: radial glia specific effect on neuronal migration. *Front Cell Neurosci* **8**, 215 (2014).

16 Wilsch-Brauninger, M., Peters, J., Paridaen, J. T. & Huttner, W. B. Basolateral rather than apical primary cilia on neuroepithelial cells committed to delamination. *Development* **139**, 95-105 (2012).

17 Askham, J. M., Vaughan, K. T., Goodson, H. V. & Morrison, E. E. Evidence that an interaction between EB1 and p150(Glued) is required for the formation and maintenance of a radial microtubule array anchored at the centrosome. *Mol Biol Cell* **13**, 3627-3645 (2002).

18 Ibi, M. *et al.* Trichoplein controls microtubule anchoring at the centrosome by binding to Odf2 and ninein. *J Cell Sci* **124**, 857-864 (2011).

19 Kodani, A., Salome Sirerol-Piquer, M., Seol, A., Garcia-Verdugo, J. M. & Reiter, J. F. Kif3a interacts with Dynactin subunit p150 Glued to organize centriole subdistal appendages. *EMBO J* **32**, 597-607 (2013).

20 Yan, X., Habedanck, R. & Nigg, E. A. A complex of two centrosomal proteins, CAP350 and FOP, cooperates with EB1 in microtubule anchoring. *Mol Biol Cell* **17**, 634-644 (2006).

21 Tanaka, N., Meng, W., Nagae, S. & Takeichi, M. Nezha/CAMSAP3 and CAMSAP2 cooperate in epithelial-specific organization of noncentrosomal microtubules. *Proc Natl Acad Sci U S A* **109**, 20029-20034 (2012).

22 Tsai, J. W., Lian, W. N., Kemal, S., Kriegstein, A. R. & Vallee, R. B. Kinesin 3 and cytoplasmic dynein mediate interkinetic nuclear migration in neural stem cells. *Nat Neurosci* **13**, 1463-1471 (2010).

23 Meng, W. & Takeichi, M. Adherens junction: molecular architecture and regulation. *Cold Spring Harb Perspect Biol* **1**, a002899 (2009).

24 Gregory, W. A., Edmondson, J. C., Hatten, M. E. & Mason, C. A. Cytology and neuron-glial apposition of migrating cerebellar granule cells in vitro. *J Neurosci* **8**, 1728-1738 (1988).

25 Nulty, J., Alsaffar, M. & Barry, D. Radial glial cells organize the central nervous system via microtubule dependant processes. *Brain Res* **1625**, 171-179 (2015).

26 Itoh, Y. *et al.* Scratch regulates neuronal migration onset via an epithelial-mesenchymal transition-like mechanism. *Nat Neurosci* **16**, 416-425 (2013).

27 Zander, M. A., Burns, S. E., Yang, G., Kaplan, D. R. & Miller, F. D. Snail coordinately regulates downstream pathways to control multiple aspects of mammalian neural precursor development. *J Neurosci* **34**, 5164-5175 (2014).

28 Sahu, S. K. *et al.* JNK-dependent gene regulatory circuitry governs mesenchymal fate. *EMBO J* **34**, 2162-2181 (2015).

29 Tiwari, N. *et al.* Sox4 is a master regulator of epithelial-mesenchymal transition by controlling Ezh2 expression and epigenetic reprogramming. *Cancer Cell* **23**, 768-783 (2013).

30 Cooper, J. A. Molecules and mechanisms that regulate multipolar migration in the intermediate zone. *Front Cell Neurosci* **8**, 386 (2014).

31 Betizeau, M. *et al.* Precursor diversity and complexity of lineage relationships in the outer subventricular zone of the primate. *Neuron* **80**, 442-457 (2013).

32 Lancaster, M. A. *et al.* Guided self-organization and cortical plate formation in human brain organoids. *Nat Biotechnol* **35**, 659-666 (2017).

33 Lancaster, M. A. *et al.* Cerebral organoids model human brain development and microcephaly. *Nature* **501**, 373-379 (2013).

34 Petry, S. & Vale, R. D. Microtubule nucleation at the centrosome and beyond. *Nat Cell Biol* **17**, 1089-1093 (2015).

35 Yonezawa, S., Shigematsu, M., Hirata, K. & Hayashi, K. Loss of gamma-tubulin, GCP-WD/NEDD1 and CDK5RAP2 from the Centrosome of Neurons in Developing Mouse Cerebral and Cerebellar Cortex. *Acta Histochem Cytochem* **48**, 145-152 (2015).

36 Sakakibara, A. *et al.* Dynamics of centrosome translocation and microtubule organization in neocortical neurons during distinct modes of polarization. *Cereb Cortex* **24**, 1301-1310 (2014).

37 Zhang, X. *et al.* Cell-Type-Specific Alternative Splicing Governs Cell Fate in the Developing Cerebral Cortex. *Cell* **166**, 1147-1162 e1115 (2016).

38 Stiess, M. & Bradke, F. Neuronal polarization: the cytoskeleton leads the way. *Dev Neurobiol* **71**, 430-444 (2011).

39 Maiden, S. L., Petrova, Y. I. & Gumbiner, B. M. Microtubules Inhibit E-Cadherin Adhesive Activity by Maintaining Phosphorylated p120-Catenin in a Colon Carcinoma Cell Model. *PLoS One* **11**, e0148574 (2016).

40 Dong, C. *et al.* CAMSAP3 accumulates in the pericentrosomal area and accompanies microtubule release from the centrosome via katanin. *J Cell Sci* **130**, 1709-1715 (2017).

41 Meng, W., Mushika, Y., Ichii, T. & Takeichi, M. Anchorage of microtubule minus ends to adherens junctions regulates epithelial cell-cell contacts. *Cell* **135**, 948-959 (2008).

42 Toya, M. *et al.* CAMSAP3 orients the apical-to-basal polarity of microtubule arrays in epithelial cells. *Proc Natl Acad Sci U S A* **113**, 332-337 (2016).

43 Taverna, E. *et al.* Non-canonical features of the Golgi apparatus in bipolar epithelial neural stem cells. *Sci Rep* **6**, 21206 (2016).

44 Burute, M. *et al.* Polarity Reversal by Centrosome Repositioning Primes Cell Scattering during Epithelial-to-Mesenchymal Transition. *Dev Cell* **40**, 168-184 (2017).

45 Obino, D. *et al.* Actin nucleation at the centrosome controls lymphocyte polarity. *Nat Commun* **7**, 10969 (2016).

46 Garcez, P. P. *et al.* Cenpj/CPAP regulates progenitor divisions and neuronal migration in the cerebral cortex downstream of Ascl1. *Nat Commun* **6**, 6474 (2015).

47 Insolera, R., Bazzi, H., Shao, W., Anderson, K. V. & Shi, S. H. Cortical neurogenesis in the absence of centrioles. *Nat Neurosci* **17**, 1528-1535 (2014).

48 Falk, S. *et al.* Time-Specific Effects of Spindle Positioning on Embryonic Progenitor Pool Composition and Adult Neural Stem Cell Seeding. *Neuron* **93**, 777-791 e773 (2017).

49 Shinohara, H., Sakayori, N., Takahashi, M. & Osumi, N. Ninein is essential for the maintenance of the cortical progenitor character by anchoring the centrosome to microtubules. *Biol Open* **2**, 739-749 (2013).

50 Sims-Mourtada, J. C. *et al.* The human AKNA gene expresses multiple transcripts and protein isoforms as a result of alternative promoter usage, splicing, and polyadenylation. *DNA Cell Biol* **24**, 325-338 (2005).

Figure Legends:

Figure 1. Akna is a centrosome component restricted to specific subtypes in the developing cerebral cortex. a, Immuno-staining of primary E14 cerebral cortex cells showing Akna at the mother centriole together with the distal-subdistal appendage maker Odf2 and the cilia and centriole marker GT335. **b**, Micrograph of E14 cerebral cortex sections showing Akna+ centrosomes at the apical, ventricular surface of the ventricular zone (VZ) and in the subventricular zone (SVZ). Very few Akna+ centrosomes are detectable in the cortical plate (CP). Pericentrin (Pcnt) labels all centrosomes throughout the cortex. Blue arrows show Pctn+ Akna+ centrosomes, red arrows Pcnt+ Akna- centrosomes. Notice that only subsets of centrosomes show Akna labelling at the apical surface of the VZ. V: Ventricle. **c**, Quantification of the distribution of Akna+ centrosomes in the E14 CTX (n=3). Data are presented as mean ± standard error of the mean. Scale bars: 2.5 μm (**a**), 20 μm (**b**).

Figure 2. Akna regulates NSC delamination and seeding of SVZ. a, Confocal micrographs illustrating binning and the distribution of control electroporated GFP+ cells 2 days after IUE. **b,** Confocal micrograph showing the distribution of GFP+ cells after knockdown of Akna using sh1. **c,** Line graph illustrating the distribution of GFP+ cells after IUE for control (green), sh1- (orange) and sh2-mediated knockdown (KD) of Akna (magenta). The respective standard error of the mean (SEM) is indicated as transparent band in the same colour (n=5 each condition). **d,** Boxplot showing the increase in Pax6+ NSCs and decrease of Tbr2+ BPs after Akna KD (n=5 each condition). **e, f,** Confocal micrographs illustrating binning and the distribution of GFP+ cells 1 day after IUE with control (**e**) or Akna overexpressing (OE) plasmids (**f**). **g,** Line graph illustrating the distribution of GFP+ cells after control (green) and Akna OE (blue) IUE with SEM as transparent band (n=5 each condition). **h, i,** Boxplots showing the decrease of Pax6+ NSCs (**h**), proliferating (Ki67+) cells (**i**) and increase in NeuN+ neurons (**h**) after Akna OE (n=5(**h**), n=4(**i**) each condition). **j,** Boxplot depicting the identity of E14 primary cortical cells transfected *in vitro*. Note that Akna OE does not elicit fate changes *in vitro* (n=3 each condition). **k,** Model describing the expression and functional role of Akna in delamination and seeding of the SVZ. Scale bars: 50 μm (**a,b,e,f**). (Mann-Whitney U test; *P < 0.05, **P < 0.01, ***P <0.001)

Figure 3. Akna regulates microtubule organization in neural progenitors. a, Example images of control or Akna shRNA2 transfected primary E14 cortical cells in nocodazole

based MT re-polymerization assays. The yellow dashed line indicates a cell in which MTs did not grow upon Akna knockdown. Boxplot showing reduced number of cells regrowing MTs at the centrosome (**b**) and reduced length of MTs (**c**) (n=4) after Akna KD (co: 110 MT endpoints, sh2: 92 MT endpoints). **d**, Ectopic Akna foci induced by Akna OE organize MT independent of centrosomes (see also Extended Data Fig. 6b). **e-h**, Akna OE in the cerebral cortex *in vivo* influences both the orientation (**e-g,** co: 117 EB3-comets, Akna OE: 122 EB3-comets in 3 experiments) and speed (**h,** co: 178 EB3-comets, Akna OE: 113 EB3-comets) of MT polymerization monitored by live imaging of EB3-GFP in cortical slices 1 day after IUE. **i**, Speed of MT polymerization is reduced in shRNA mediated knockdown in vivo (sh (co): 56 EB3-comets, sh1(Akna): 96 EB3-comets). (Mann-Whitney U test; * $P < 0.05$, ** $P < 0.01$, *** $P < 0.001$). Scale bars: 5 μm.

Figure 4. EMT progression requires Akna to dissolve junctional coupling. Micrographs of NMuMG cells immunostained in untreated (**a**) and TGF-beta-1-treated EMT inducing conditions with control (**b**) or Akna siRNA (**c**). Staining for ZO1 (**a', b', c'**) shows that junctional coupling dissolves only in control TGF-beta-1 induced EMT, but not when treated with Akna siRNA. Phalloidin (**a'', b'', c''**) stainings reveal that the redistribution of Actin filaments from junctions to cytoplasm during EMT is affected upon Akna KD. **d,e**, Confocal micrographs of electroporated cortices 18h after IUE depict examples of GFP+ cells with reduced levels of E-Cadherin upon Akna OE. Scale bars: 10 μm (**a-c**), 20μm (**d,e**).

Figure 5. Akna regulates retention of cells within the SVZ. a,b, Confocal micrographs illustrating binning and the distribution of electroporated cells expressing GFP+ (**a**) or Akna and GFP (**b**) under the control of the Dcx promoter 5 days after IUE **c,** Line graph illustrating the distribution of GFP+ cells after IUE for control (green), and Akna OE (blue) with SEM indicated as transparent band (Dcx-GFP: n=5; Dcx-Akna n=4). **d,** Boxplot showing the fraction of GFP+ cells retained below the CP labelled by Tbr1 (Dcx-GFP: n=5; Dcx-Akna n=3). **e,** Dotplot overlayed with a Violin plot showing the distribution of migration speed of control and Akna KD neurons assessed during live imaging in slices 2 days after IUE. The mean ± SEM is indicated in bold (Dcx-mirR(neg): n=34; Dcx-mirR(Akna): = 26). **f-i,** Boxplots illustrating the morphology transitions of control and Akna KD cells (**f,g**) of after Akna OE (**h,i**) (Dcx-miR(neg) n=2; Dcx-miRNA(Akna) n=3; Dcx-GFP n=3 and Dcx-Akna n=3). Scale bars: 50 μm (**a,b**). (**c,d,e**: Mann-Whitney U test; *$P < 0.05$; **f-i**: Students t-Test*$P < 0.05$, **$P < 0.01$)

Extended Data Figure 1. Akna expression, centrosome localization and antibody verification. a, RT-qPCR data show higher levels of Akna mRNA in E14 than E11 or E18 cerebral cortex (n=3). **b**, Microarray data depicting higher Akna expression in NSCs that generate neurons via BPs (CD133+/GFPhigh)[6] (n=3). **c**, WB of Akna in E14 cerebral cortex lysate running at higher than predicted (153 kD) molecular weight due to phosphorylation (data not shown, see also Extended Data Fig. 3d). **d**,**e**, WB of Akna in Neuro2a cell lysates after transfection with Akna sh1 and sh2 or control (**d**) or 3 different miRNAs and control (**e**) using the antibody clone 14D7. **f**, Akna IF using clone 25F1 in primary E14 cortical cells showing Tbr2+ BPs lacking Akna IF signal upon transfection with Akna siRNAs but not in control, showing specificity of the immunostaining. **g**, IF of Akna and Tubg1 in primary E14 cortical cells showing Akna signal surrounding a single Tubg+ centriole. **h**, A20 BAC transgenic cell line showing GFP-tagged Akna at centrosomes marked by Tubg in interphase (**h'** and **h'''**), but not during mitosis (**h''**). **i**, Predicted domains of murine Akna protein. **j**, Amino acid sequence of Akna's AT-hook containing transcription factor domain and the AT-hook-like domain. Notice that neither has the GRP-core sequence surrounded by several K/R amino acids, which is required for DNA or RNA-binding AT-hook domains, such as the AT-hook domains of Hmga1. **k**, WB of Akna in nuclear and cytoplasmic cell fractions of A20 cells showing Akna signal in the cytoplasm only. **l**, Mass-spectrometric analysis of sucrose gradient-based isolated cellular sub-fractions of A20 cells. Akna is enriched in fractions 3 and 4 containing the centrosomal components listed on the right side. **m**-**o**, Immunostaining of dissociated hiPSC-derived cerebral organoid cells showing AKNA localization at centrosomes with three different monoclonal antibodies. Clone 9G1 and 4F5 recognize epitopes at the N- and C-terminal part of the protein, respectively, suggesting that different splice variants[8,50] still localize at centrosomes. Also notice the enrichment at one (mother) centriole. * $P < 0.05$, *** $P < 0.001$. Scale bars: 5 μm (**f, h, m, n, o**), 2.5 μm (**g**).

Extended Data Figure 2. Mechanisms localizing Akna at the subdistal appendages. a, b, EM micrographs showing Akna immunogold-labeling at SDAs in the SVZ (**a**) and VZ (**b**) of E13 cerebral cortex sections with (**b'**) as magnification of the boxed area showing SDA in (**b**). **c**, STED nanoscopy picture showing Akna IF signal surrounding Odf2 IF signal showing more distal localization of Akna at the SDA, while Odf2 localizes proximal in respect to the centriole in E14 brain NSCs as summarized in the schematic drawing below (Akna indicated in green, Odf2 in magenta). **d**, Schematic drawing of different truncated Akna variants used to analyze the sub-cellular localization as indicated to the right. **e**-**h**, Micrographs showing the localization of the truncated Akna forms expressed in primary E14 cortical cells. The constructs containing the last 370 amino acids (**f, h**) localize to centrosomes. Otherwise IF signal is observed in the cytoplasm (**e, g**) and in the nucleus (**e**). Notably, the clone used in Siddiqa et al.,[8] lacked the c-terminal centrosome targeting part. **i**-**k,** E14 primary cortical cells

treated with DMSO (**i**), nocodazole (**j**) or Dctn2 overexpression (**k**) show Akna IF remaining at centrosomes. **l**, Micrographs showing Akna IF signal at centrosomes at the apical, ventricular surface in sections of E15 WT, but not *Sas4*$^{-/-}$ *p53*$^{-/-}$ mice lacking centrioles[47]. Note that Pcnt+ pericentriolar material remains present in the absence of centrioles *Sas4*$^{-/-}$ *p53*$^{-/-}$ mice. **m, n**, Akna IF of WT (**m**) or Crispr-Cas9 generated *Odf2*-KO (**n**) mammary epithelial cells showing that Akna is lost from centrioles lacking SDAs. Altogether, the data demonstrates that Akna is an internal component of SDAs and is not recruited to centrosomes by MT or Dynein/Dynactin motors. Scale bars: 0.1 μm (**a, b, c**), 10 μm (**e, g, h, l, m, n**), 5 μm (**f,i,j,k**).

Extended Data Figure 3. Akna dissociates from the centrosome in mitosis depending and due to increased phosphorylation. a, IF of Akna in primary E14 cortical cells at different phases of the cell cycle showing lack of Akna IF at the centrosome during mitosis. **b**, WB of Akna in synchronized A20 cells showing that Akna protein is not degraded during mitosis indicated by the presence of phospho-Histone H3. **c**, Representative micrographs of Akna and Pcnt IF in E14 primary cortical cells. Akna IF is observed at centrosomes at 0 hours, but is it is undetectable 3 hours after treatment with protein phosphatase inhibitor okadaic acid (OA). This shows that centrosomal localization is phosphorylation-dependent. **d**, WB of lysates of OA treated cells showing that phosphorylation, here caused by protein phosphatase inhibition, delays Akna protein migration on SDS-PAGE and subsequently leads to protein degradation as observed in lysates of cells 5 hours after OA washout. Scale bars: 5 μm (**a**), 10 μm (**c**).

Extended Data Figure 4. Temporal and sub-type specific regulation of Akna in the developing telencephalon. a-c, Micrographs showing that Pcnt+ centrosomes lack Akna in the cerebral cortex at E9 (**a**) and E18 (**b**) while Akna is enriched in the VZ and, specifically, the SVZ at E14 in the ganglionic eminence (**c**) and the cerebral cortex (Fig. 1). **d-f**, Histograms showing the percentage of Akna+ centrosomes in E14 cerebral cortex regions (**d,e,** n=3) as indicated and in dissociated primary E14 cortical cells (**f**) revealing that cells with Akna+ centrosomes are mostly differentiating NSCs (Pax6-Tbr2) and Tbr2+ BPs (n=3). **g,** Micrographs of cells isolated from E14 cerebral cortex by FACS using prominin1 and stained for Pax6 (red arrows) and Tbr2 (blue arrows) showing that double positive (differentiating) NSCs have Akna+ centrosomes, while Pax6+/Tbr2-negative (proliferating) NSCs do not. Scale bars: 10 μm (**a,c,g**), 20 μm (**b**).

Extended Data Figure 5. Akna knock-down elicits cell death and delamination defects persists upon cell death rescue by p53 reduction. a-c, Micrographs showing TUNEL staining in E15 cerebral cortex indicating cell death 2 days after IUE with Akna shRNA1 (**b**) or 2 (**c**), but not with control plasmids (**a**). **d, e**, Micrographs showing the distribution of GFP+ cells in E15 cerebral cortex 2 days after IUE with control shRNA (**d**) or Akna shRNA2 plus p53-miRNA plasmids (**e**). Note that p53-downregulation rescues the apoptotic effect of Akna knock-down. **f**, Line graph illustrating the distribution of GFP+ cells in the cerebral cortex after control (green, n=6) and Akna sh2/p53 miR (purple, n=8) IUE with SEM as transparent band showing still a delamination defect upon Akna KD when cell death is blocked (sh2 + p53-miR). **g**, Boxplot showing the decrease of GFP+ Tbr2+ cells after IUE of Akna shRNA + p53-miR compared to control, showing that defects in delamination are accompanied by retaining NSC fate. (Mann-Whitney U test; **P < 0.01). Scale bars: 50 μm (**a-e**).

Extended Data Figure 6. Akna is sufficient to mediate MT polymerization and recruit g-Tubulin and SDA components. a-e, Micrographs of E14 primary cortex cells treated and immunostained as indicated. **a**, Time-series depicting regrowth of the microtubule cytoskeleton after nocodazole mediated de-polymerization. **b,** Regrowth of the microtubules 60 seconds after nocodazole mediated de-polymerization in Akna OE (GFP+) cells. Red arrows indicate centrosomes. Note that MTs polymerize also from ectopic Akna+ sites. **c,** Confocal images showing co-labeling of Akna foci with gTurC components Tubg1 and Gcp4. **d,** Akna foci fail to recruit MT minus end capping-proteins Camsap2 and the centrosomal protein Pcnt. **e,** Confocal micrographs depicting colocalization of ectopic Akna foci with the Odf2, Dctn1, and Mapre1. **f,** Co-immunoprecipitation experiments with lysates from E14 cerebral cortex, IP with Akna antibody and WB with Akna, Odf2, Dctn1, Mapre1 and Gcp2, showing that these proteins are in the same complex, except Gcp2 (i.e. the gTuRC). Scale bars: 5 μm (**a-e**).

Extended Data Figure 7. Akna regulation and function during EMT in mammary epithelial cells. a, b, Akna IF in untreated (**a**) and 1 day with TGF-beta-1 treated (**b**) NMuMG cells. Red arrows indicate Akna-negative centrosomes (Pcnt+) in untreated cells and blue arrows Akna+ centrosomes in TGF-beta-1 treated cells. **c**, WB showing Akna protein increase during the first days after EMT induction and subsequent decrease to levels in untreated cells. Coomassie-stained gel showing equal loading is shown on the right side. **d**,

WB of Akna in untreated, control and Akna siRNA transfected cells at 4 days TGF-beta-1 treatment. Note the efficient knock-down of Akna by siRNA treatment. **e**, WB of ZO1 in untreated, control and Akna siRNA transfected cells at 4 days TGF-beta-1 treatment. The middle panel is a longer exposure. Note the increased ZO1 protein levels upon Akna KD in equal loading as indicated in the lower panel. **f**, WB of p120 and phospho-p120 in untreated, control and Akna siRNA transfected cells at 4 days TGF-beta-1 treatment. (**e**) and (**f**) demonstrate that degradation of junctional proteins during EMT is blocked by Akna knockdown. In accordance, cells are less scattered in Akna knockdown conditions compared to control (**g-i**). Scale bars: 5 μm (**a**), 30 μm (**f, g, h**).

Extended Data Figure 8. Lower Akna levels in differentiating neurons mediates acentrosomal MT polymerization and allow migration into the cortical plate. a, b, Primary E14 cortical cells were sorted for Prominin1 (CD133) to isolate NSCs or PSA-NCAM to isolate neurons as indicated in the panels. Prom1+ cells express the NSC marker Nestin, while PSA-NCAM+ cells express the neuronal marker Tubb3 showing the specifity of the FACS sort (**a**). Microtubule regrowth assay in purified NSCs shows centrosomal microtubule polymerization (**b**, upper panels), purified neurons show largely non-centrosomal microtubule polymerization patterns (**b**, lower panels). **c,** Micrographs showing co-electroporation of a CAG-dsRED and Dcx-GFP at E13 and analysis at E15. Note the onset of Dcx-GFP expression (**c**'') only in the BP/neuronal compartment of the developing cortex, while DsRed+ cells are also found in the VZ (**c, c'**). **d,** Micrographs showing electroporated cells (GFP+) in control (Dcx-GFP) and **e,** Akna overexpressing (Dcx-Akna) conditions. Note that many Akna OE cells accumulate in the SVZ and are unable to migrate into the CP. **f,** Micrographs of Akna OE cells retained in the SVZ co-stained for Tbr1, Ctip2, and Cux1 labelling neurons of different layer identity. Note that the neurons accumulating below the CP upon Dcx-driven Akna contain neurons positive for each of these neuronal identities. **g,** Micrographs showing that electroporated cells (GFP+) after control and Dcx-miR driven downregulation of Akna enter the CP equally well. **h**, Line graph illustrating the distribution of GFP+ cells after IUE for control (green), and Dcx-Akna overexpression (purple). In the same color transparently underlying the line graph the respective standard error is indicated (Dcx-miR (neg): n=4; Dcx-miR4 (Akna) n=3). Scale bars: 5 μm (**a, b**); 50 μm (**c-g**).

Extended Data Figure 9. AKNA localization in ferret and macaque cerebral cortex and function in human cerebral cortex organoids. a, qPCR for AKNA showing the transient but strong upregulation of AKNA mRNA in ferret VZ tissue at E34, the time when cells forming the oSVZ leave the VZ[3]. **b**, Microarray data showing higher AKNA mRNA levels in the lateral sulcus (LC) compared to splenial gyrus (SP) in oSVZ tissue of ferret brain at P1. **c**, WB showing higher levels of AKNA protein in LS compared to SG from ferret oSVZ tissue at P1. **d**, Micrograph showing AKNA and TUBG co-localization at centrosomes in ferret brain cells at (P1). **e, f**, Comparison of AKNA IF in ferret VZ and oSVZ tissue in SP versus LS. Notice more abundant IF signal in oSVZ of LS, corresponding with mRNA and protein levels as determined by WB. Given that oSVZ of gyrus contains more basal radial glia with bipolar morphology than sulcus, we propose that AKNA levels regulate the multipolar to bipolar transition in ferret as in mouse SVZ with higher levels retaining more cells in a multipolar state (see Fig. 5f-i). **g, h**, AKNA IF in macaque germinal zone (GZ) and cortical plate (CP) at E64. Arrows indicate AKNA+ centrosomes and denote abundant IF signal. The square in (**g**) shows a representative example of a TUBG+ AKNA+ centrosome in the GZ, while the one in (**h**) depicts an AKNA-negative centrosome in the CP. **i,** Micrographs of human NPCs derived from hiPS cells overexpressing Akna showing multiple foci of MT polymerization. **j, k,** In situ hybridization (ISH) in hiPSC derived cerebral organoids showing enrichment of AKNA mRNA in non-apical SVZ-like areas. **l, m,** Micrographs showing sections of human brain organoids stained for GFP+ cells electroporated with a control plasmid (**l**) or a plasmid overexpressing the human form of Akna (**m**). **n,** Line graph illustrating the distribution of GFP+ electroporated cells after IUE for control (green) and Akna OE (blue) in 3 different culture batches (n=3). **o,** Line graph illustrating the distribution of GFP+ electroporated cells after IUE for control (green) and Akna knock down (orange) (n=3). Data are shown as mean ± SEM (**a,b**; Students t-Test *P < 0.05, ***p< 0.001; **n,o**: Mann-Whitney U test; *P < 0.05). Scale bars: 5 μm (**d**); 50 μm (**e, f, i**); 10 μm (**g, h**); 50 μm (**j, k**).

Extended Data Figure 10. Akna does not regulate cilia formation or localization. a, b, Histograms depicting the percentages of ciliated cells (Arl13+) (**a,** n=3) and short vs. long cilia (**b,** n=3) in control or Akna shRNA transfected E14 primary cortical cells. **c-d**, iCLEM micrographs of in utero electroporated cells. The images compare two neighboring NSCs; one electroporated (blue) and one non-electroporated (orange). Yellow and pink arrows show anti-GFP and anti-Tuba immunogold-signal in the cytoplasm and cilium of the electroporated cell.

706 Notice that Akna electroporation does not notably affect cilia formation *in vivo*. Scale bars: 30
707 μm (**c**-IF); 1 μm (**c**-EM); 0.1 μm (**d**).

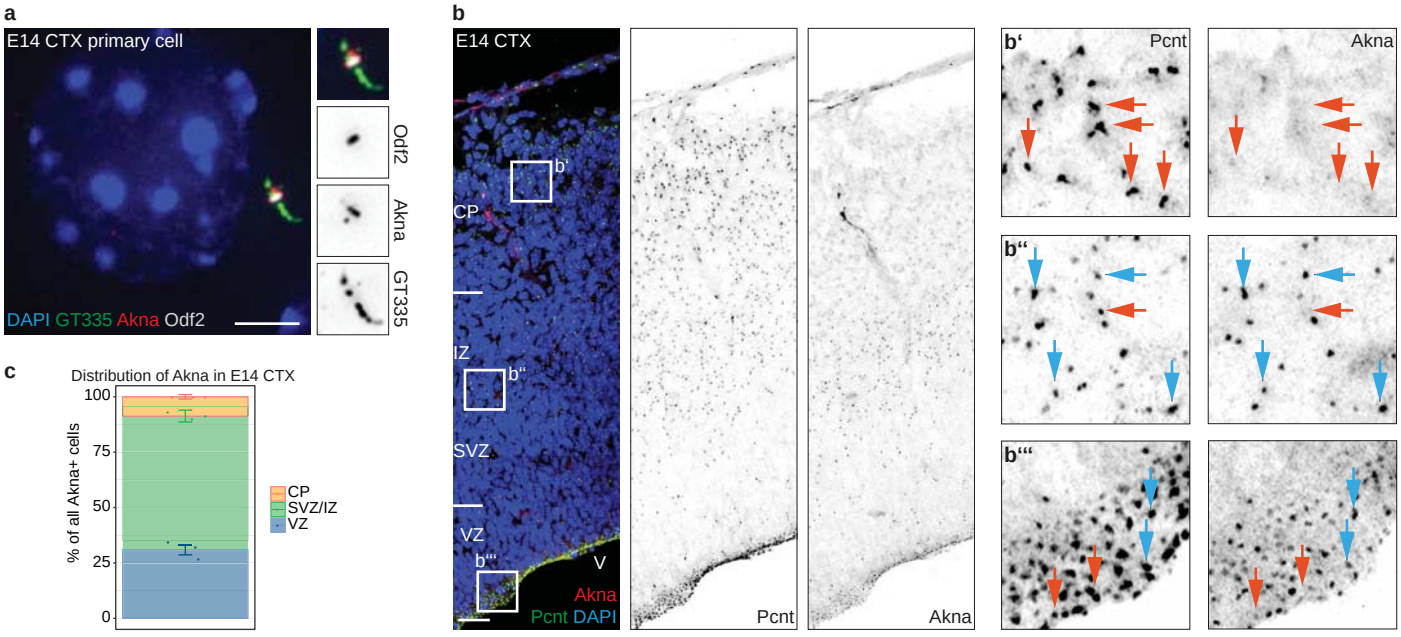

Figure 1, Camargo Ortega et al.,

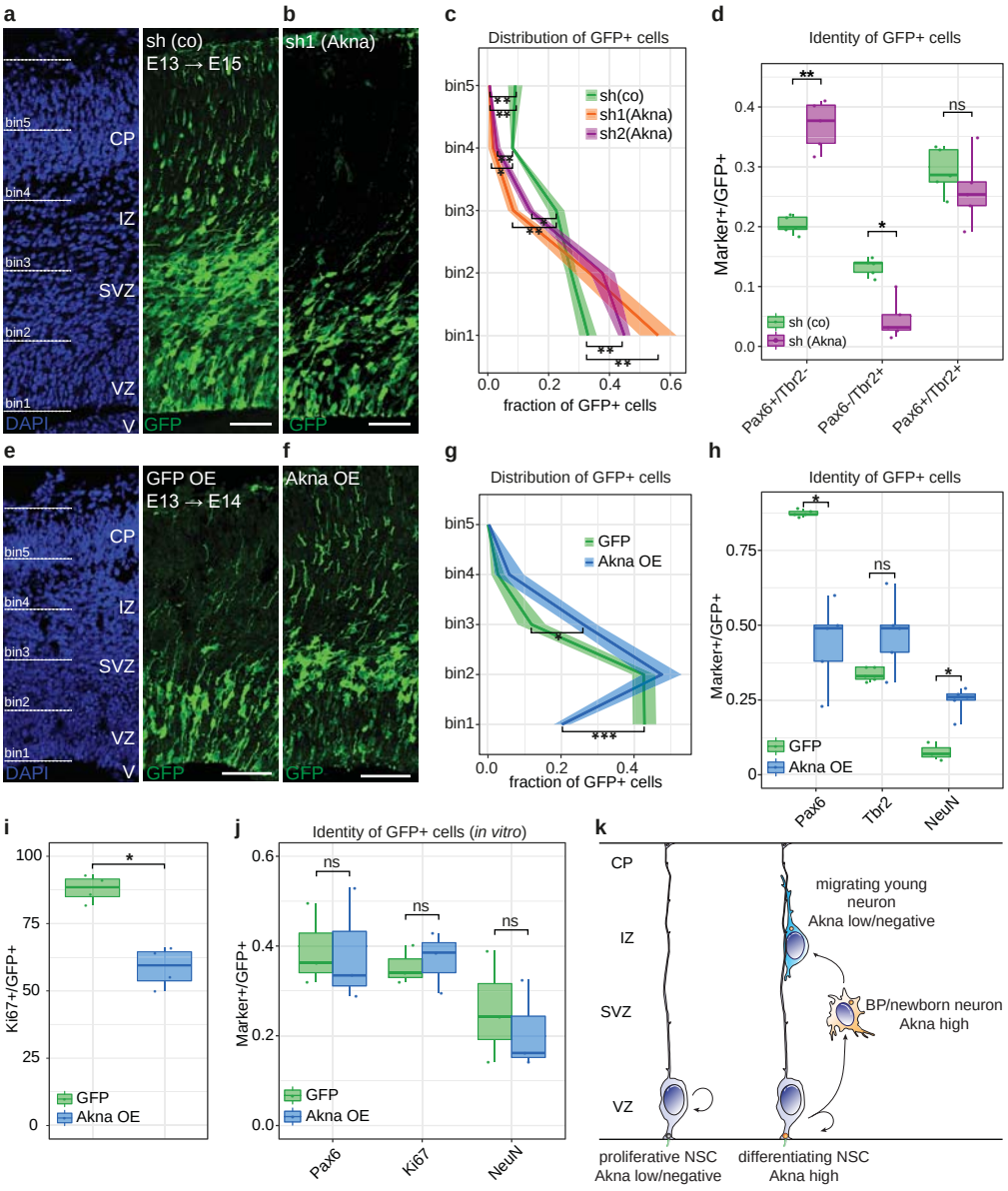

Figure 2, Camargo Ortega et al.,

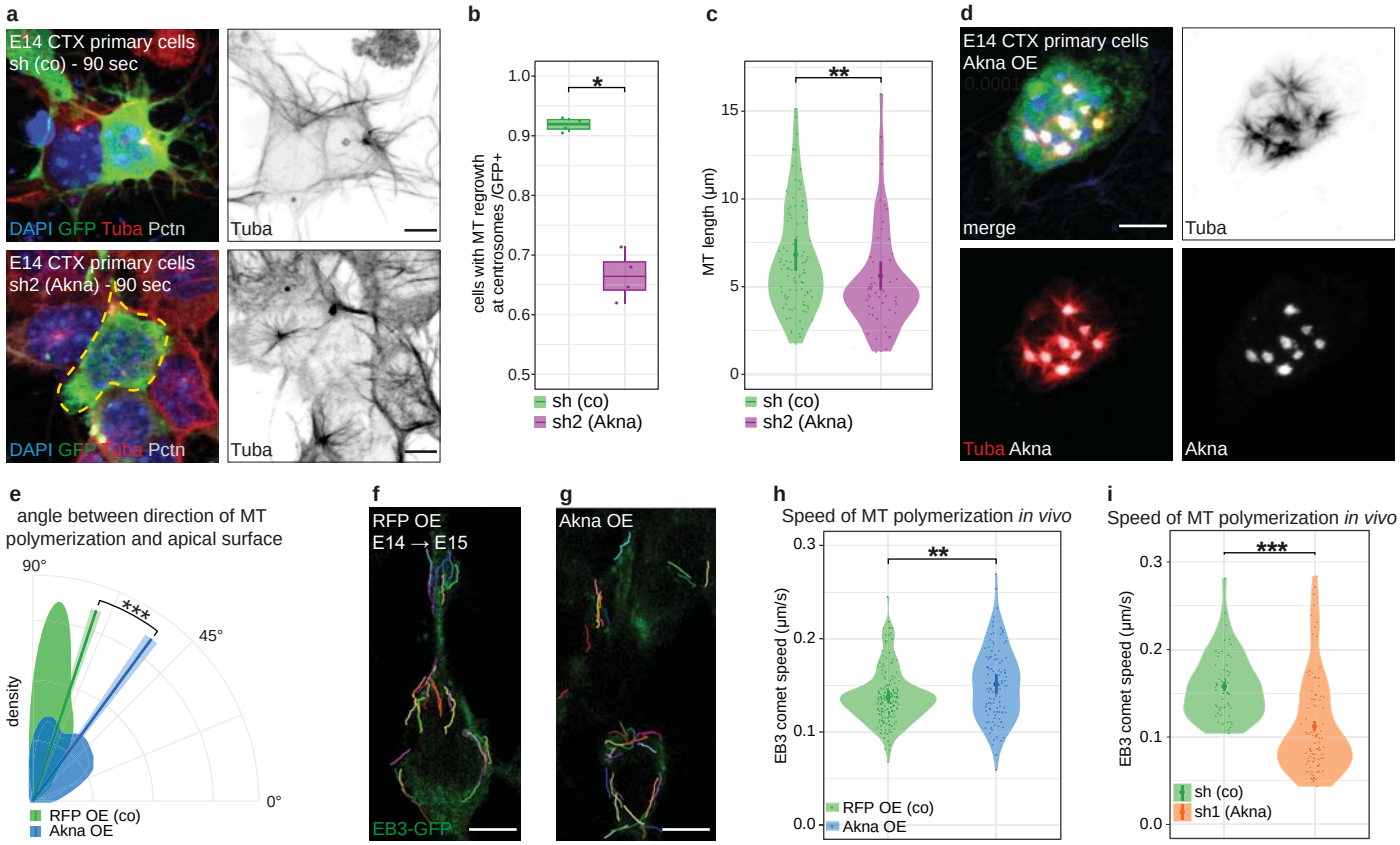

Figure 3, Camargo Ortega et al.

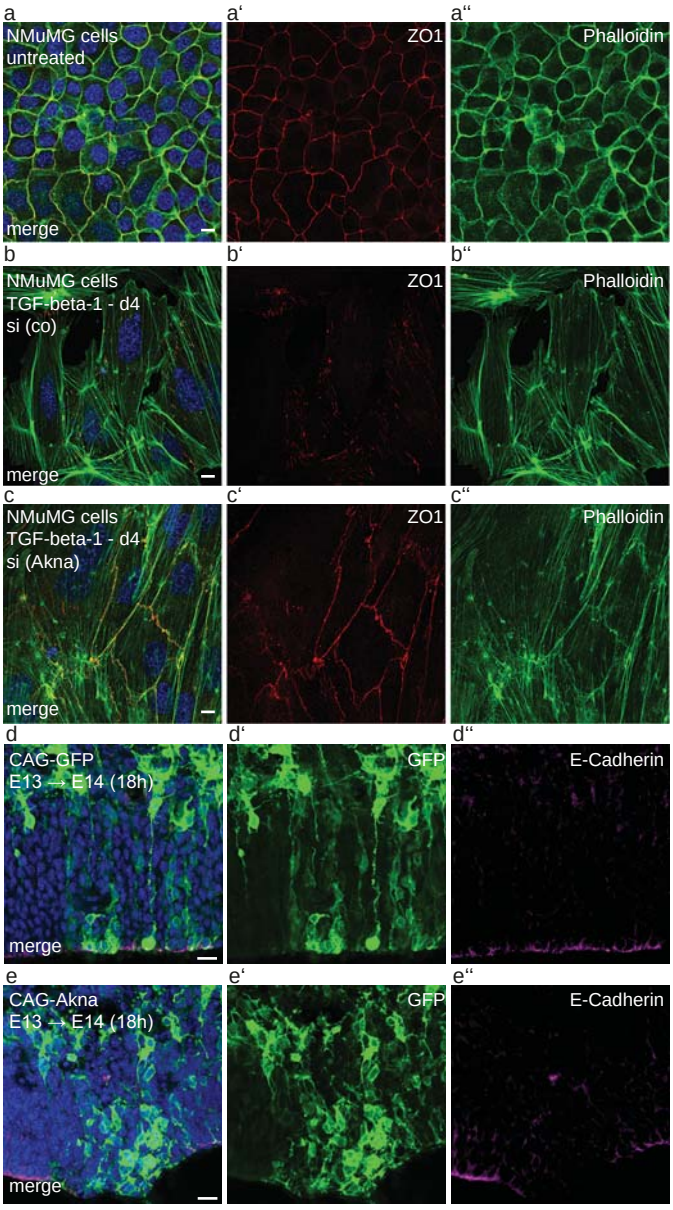

Figure 4, Camargo Ortega et al.

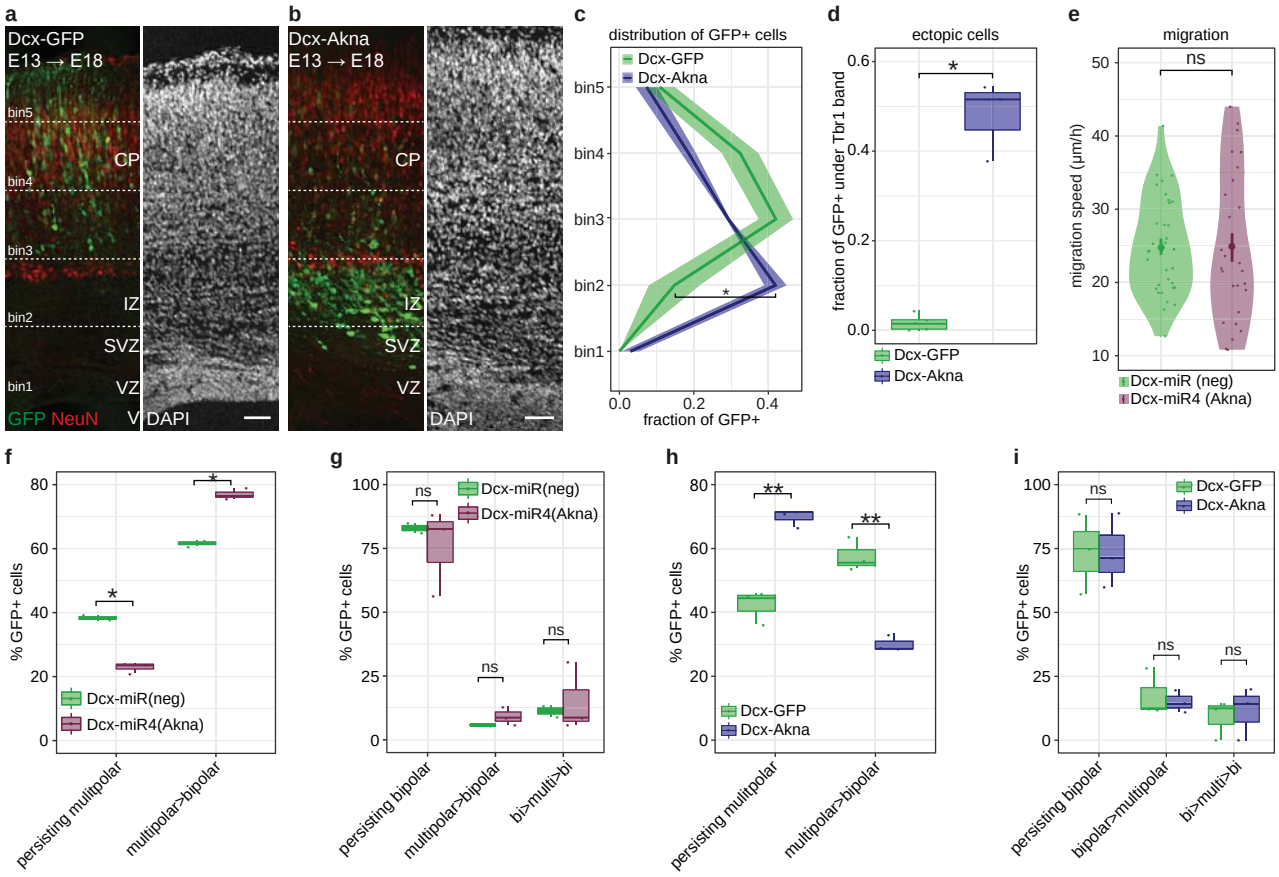

Figure 5, Camargo Ortega et al.

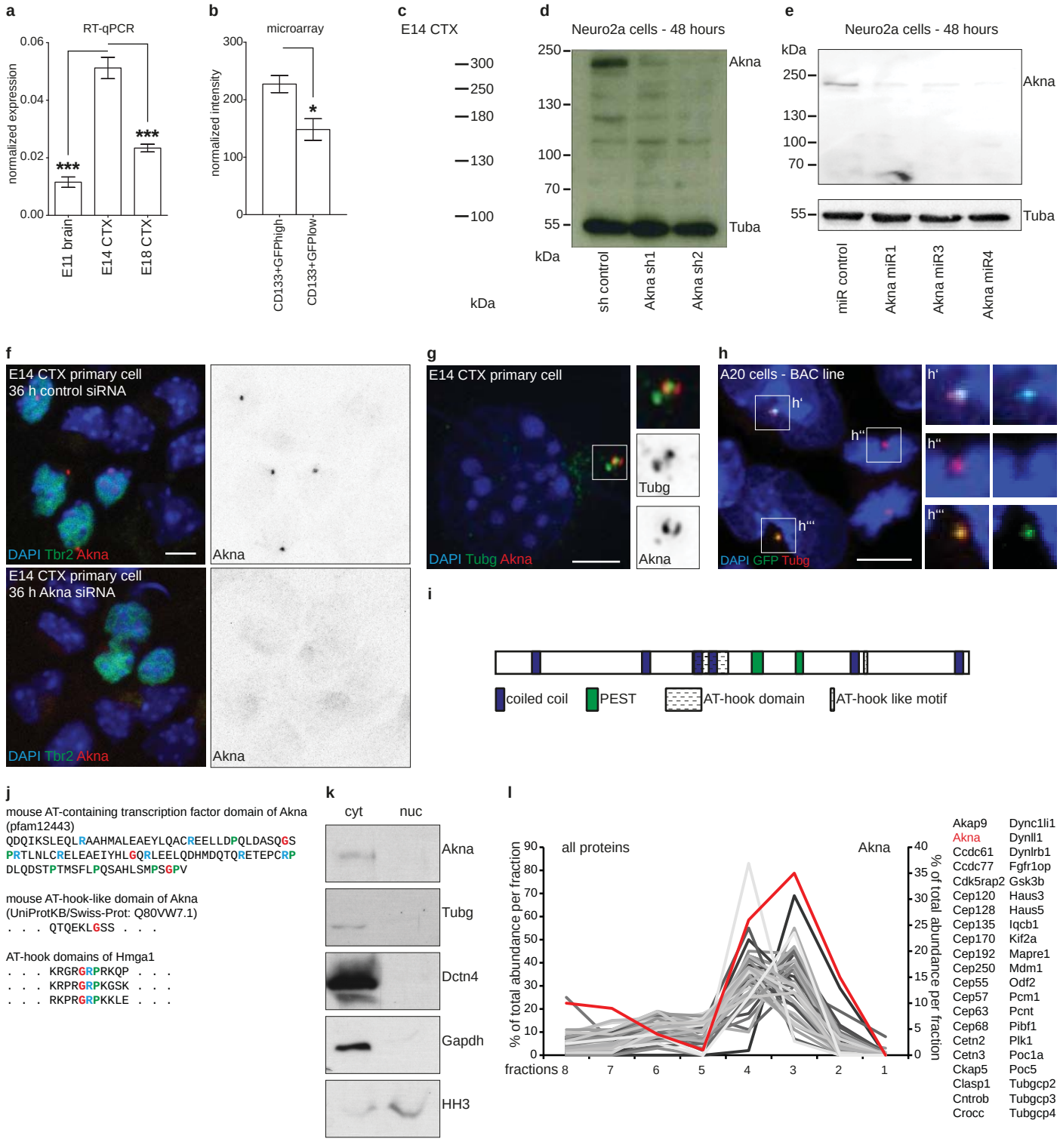

Extended Data Figure 1, Camargo Ortega et al.

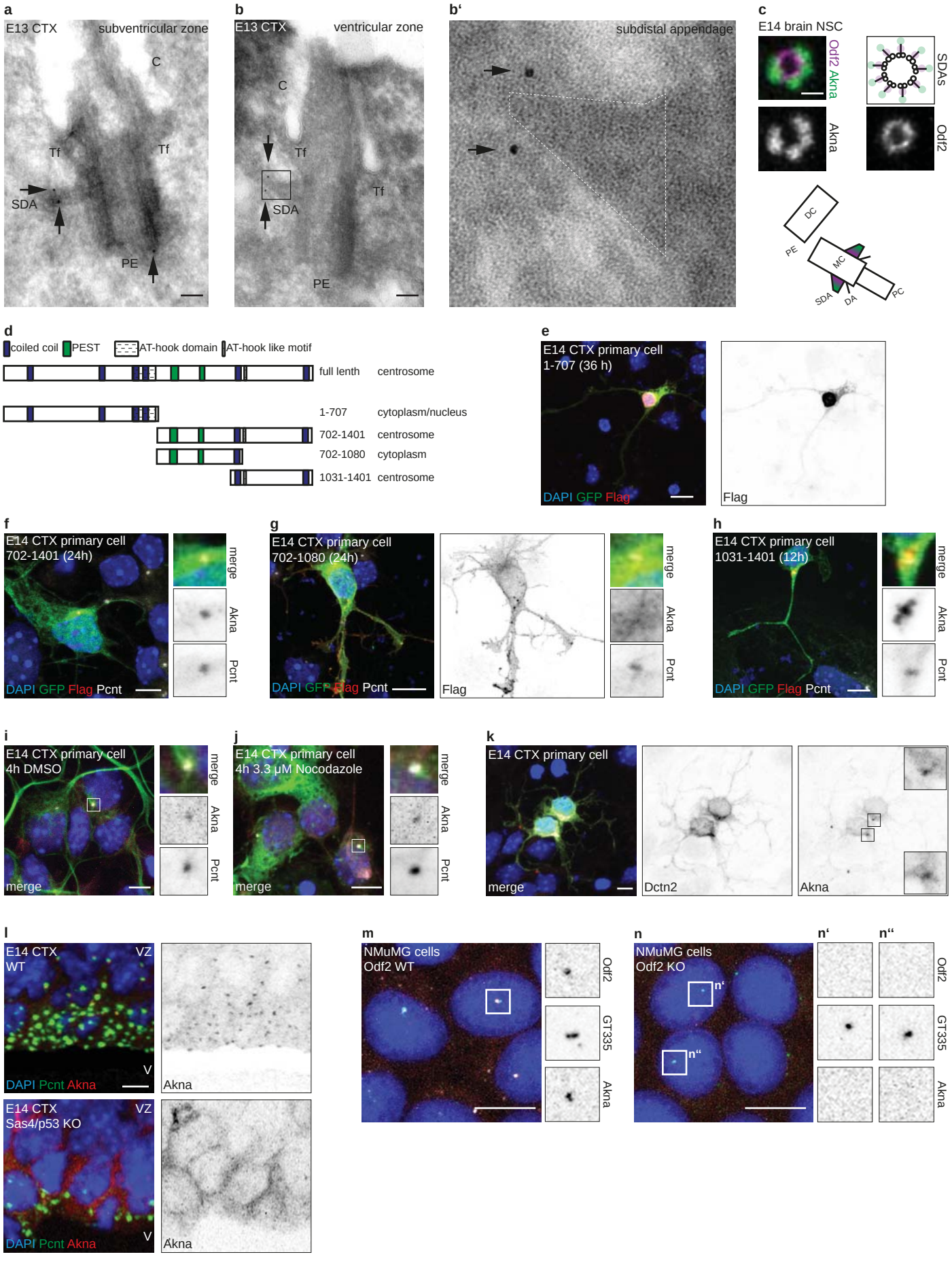

Extended Data Figure 2, Camargo Ortega et al.

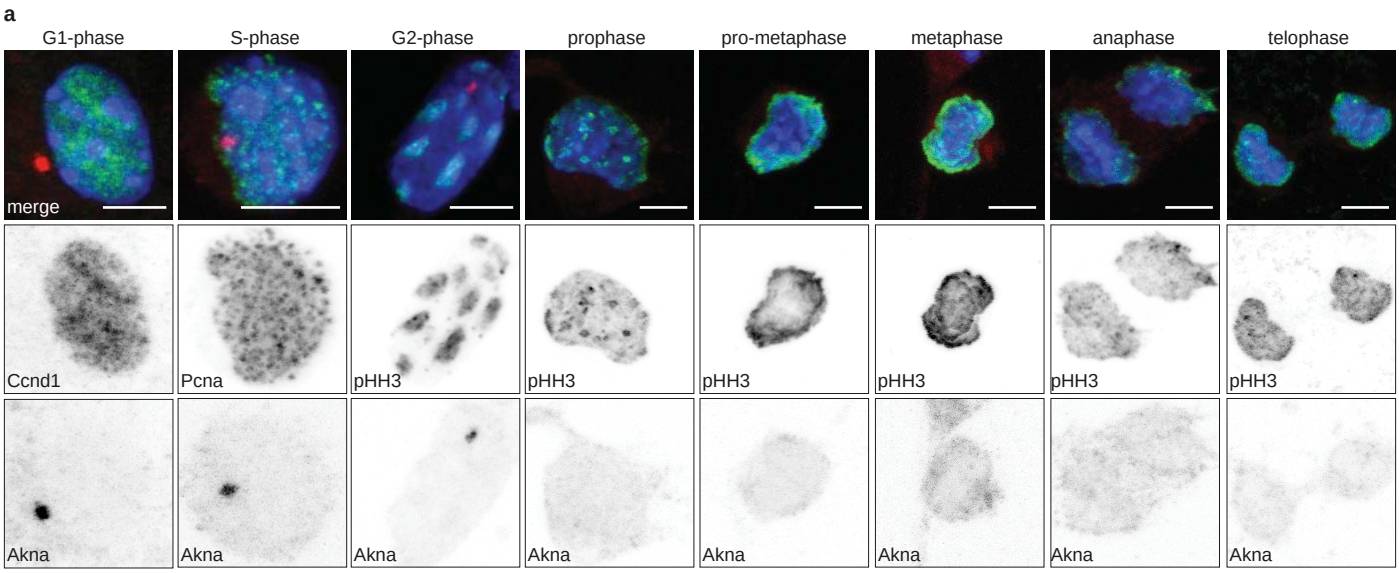

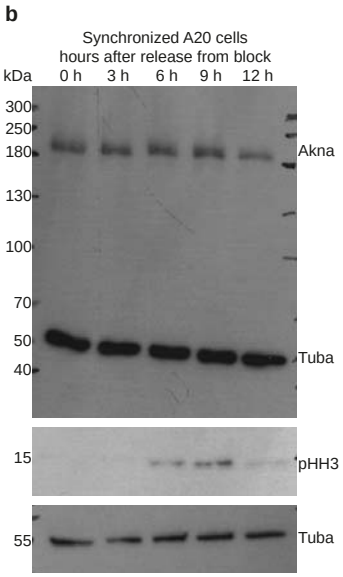

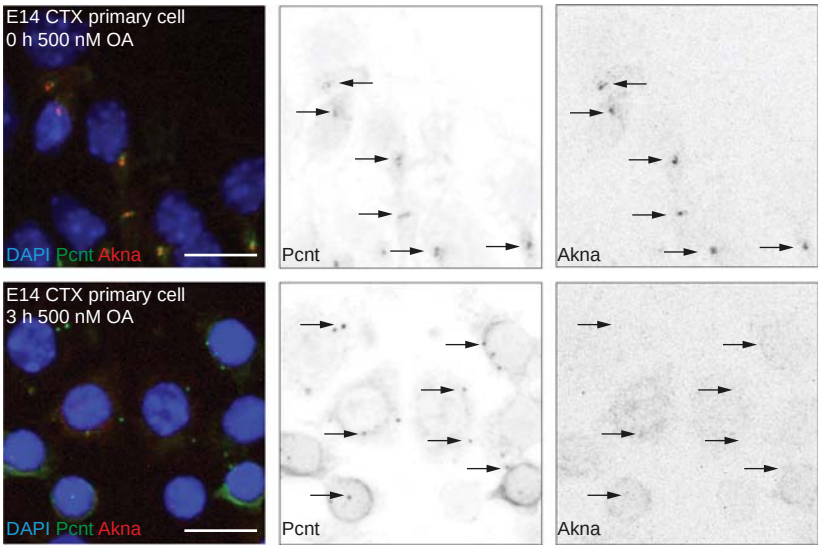

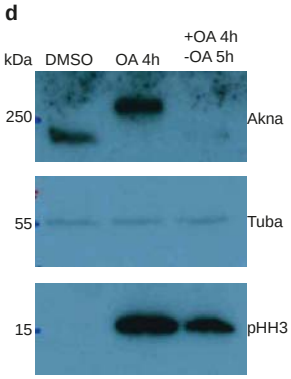

Extended Data Figure 3, Camargo Ortega et al.

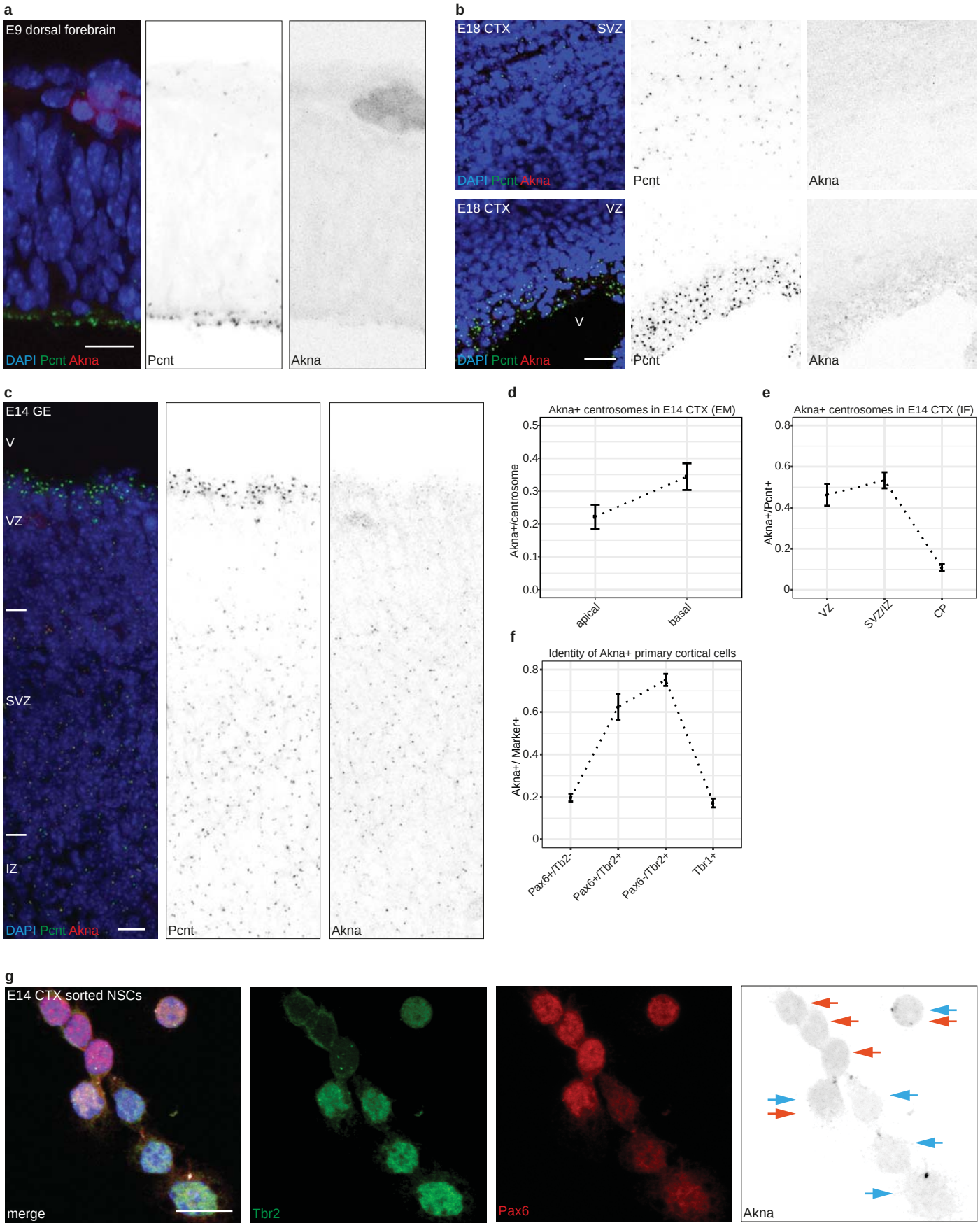

Extended Data Figure 4, Camargo Ortega et al.

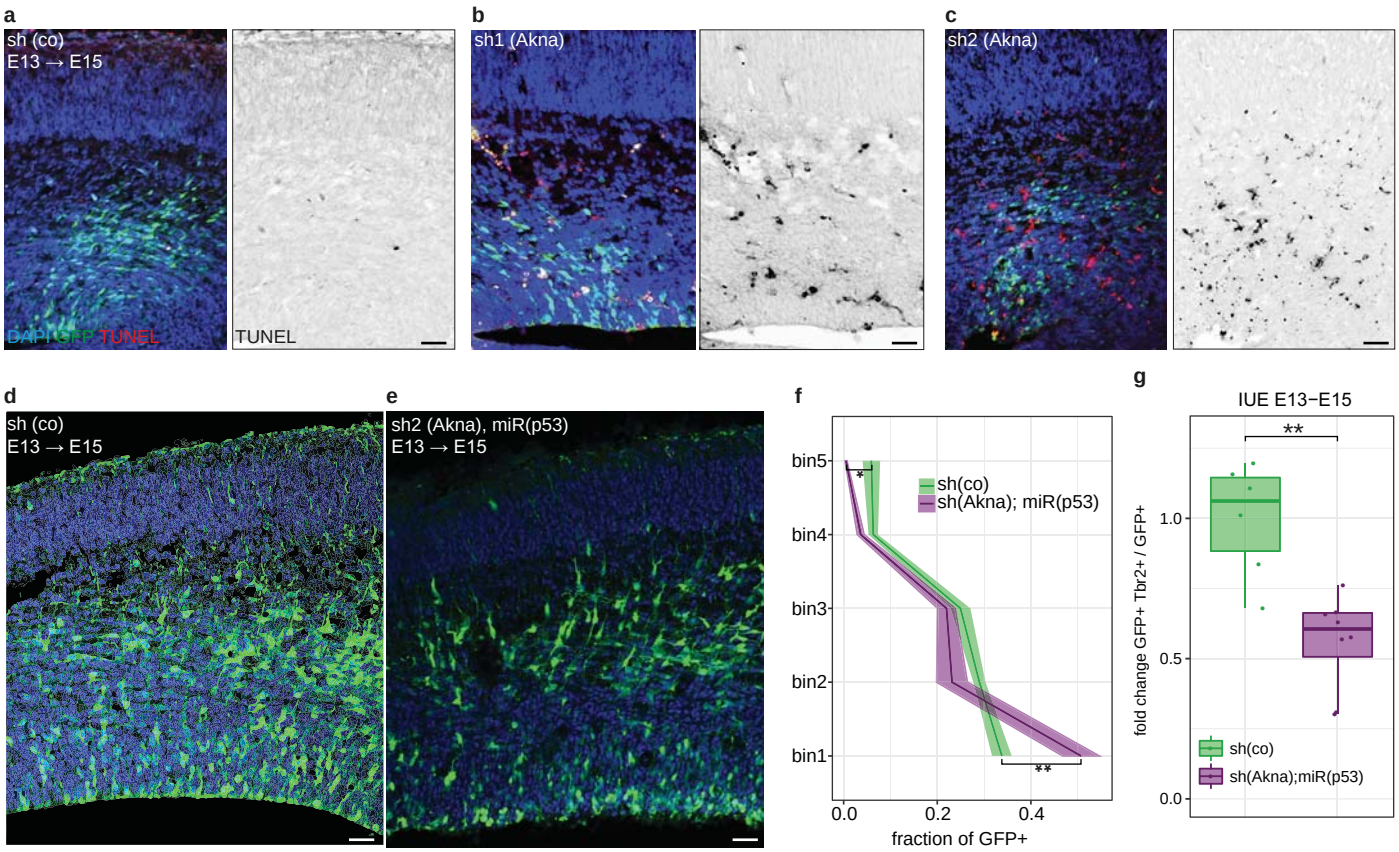

Extended Data Figure 5, Camargo Ortega et al.

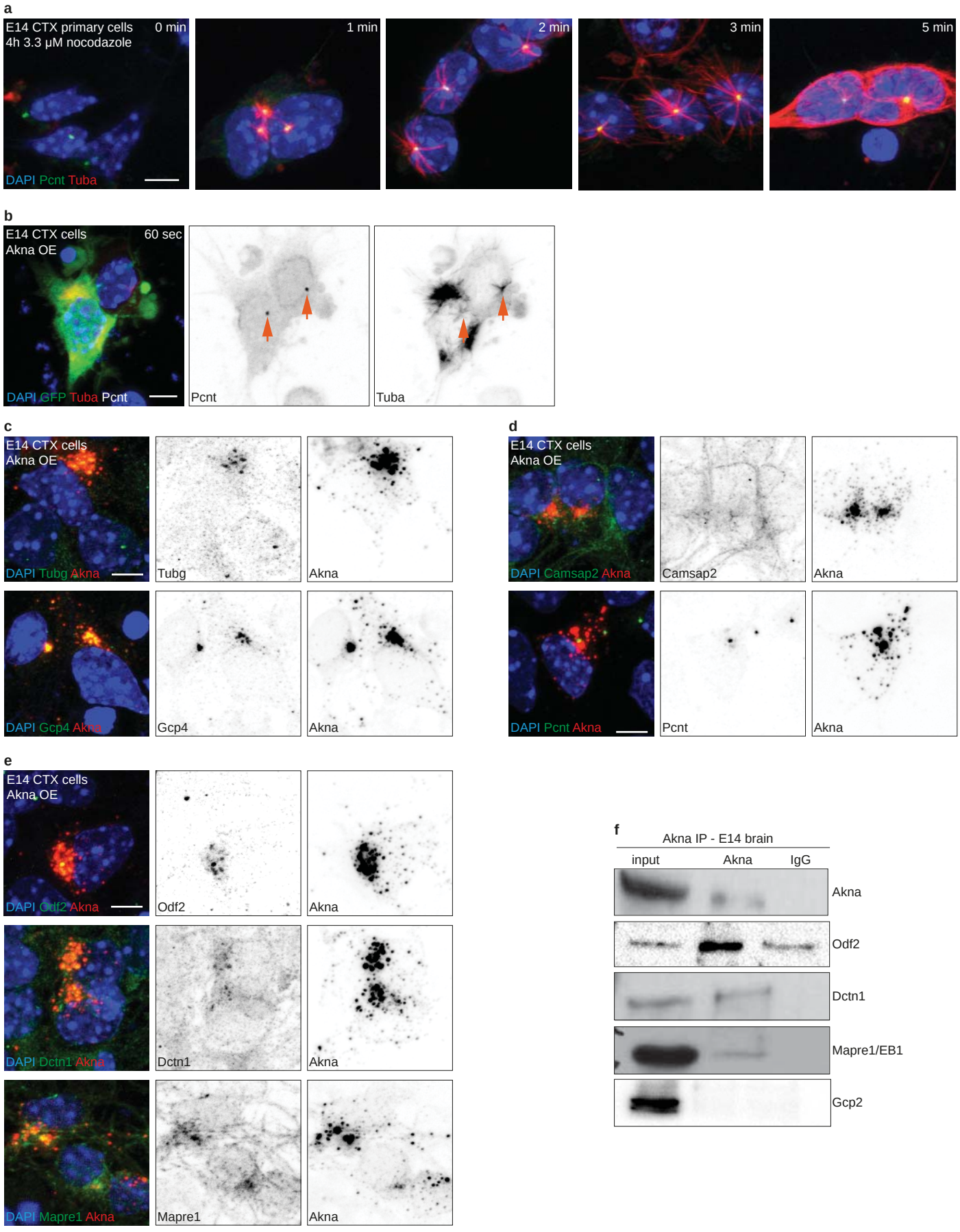

Extended Data Figure 6, Camargo Ortega et al.

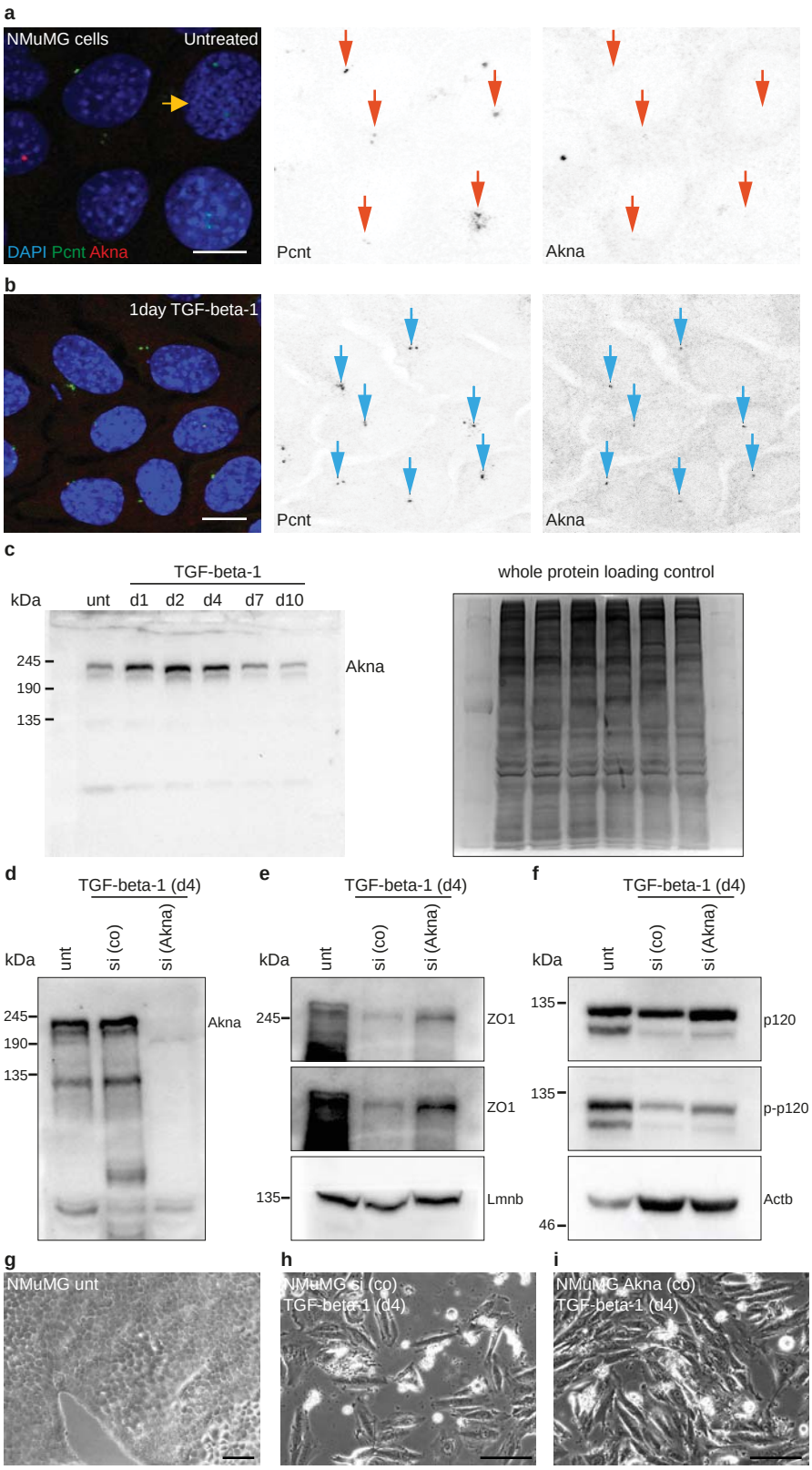

Extended Data Figure 7, Camargo Ortega et al.

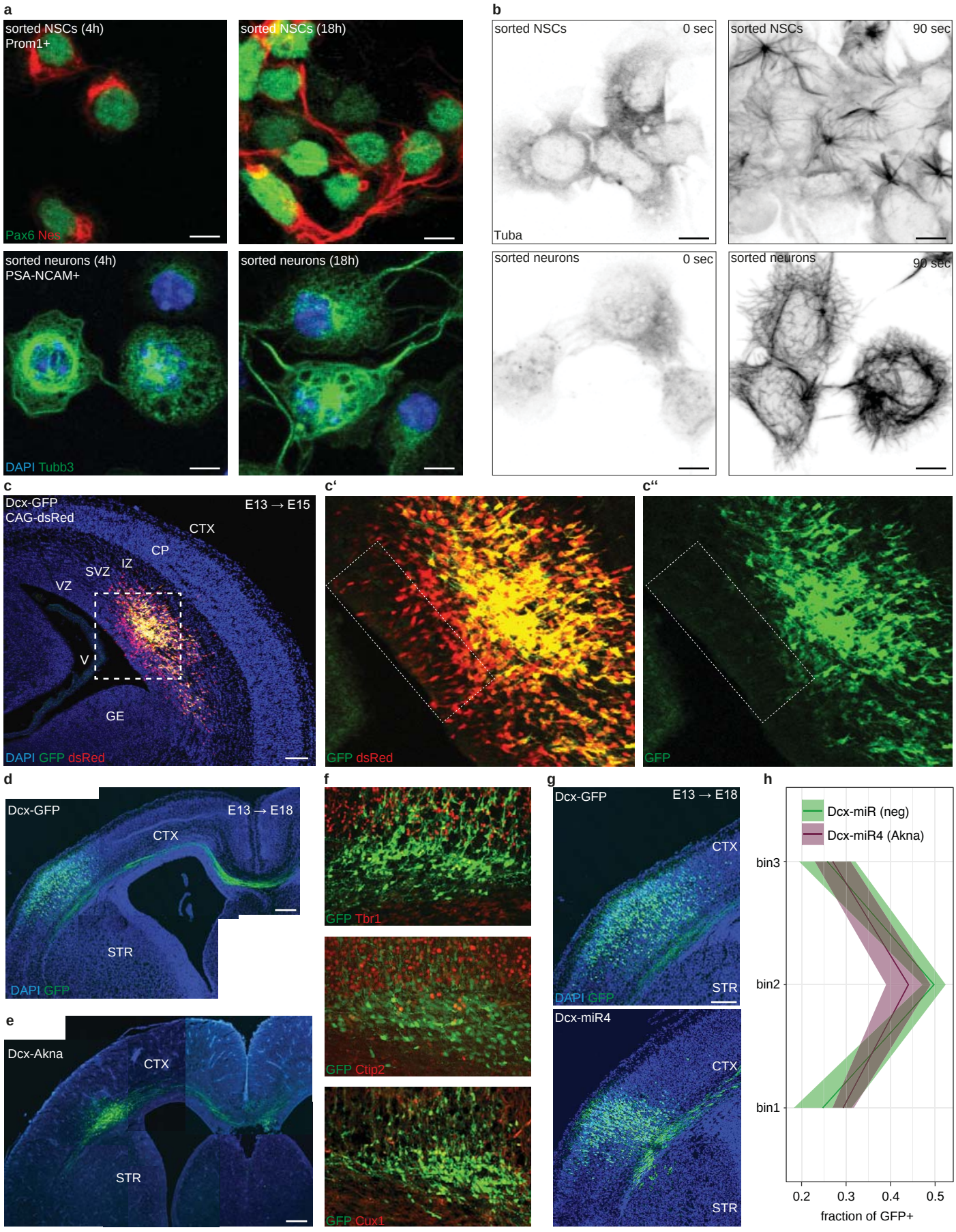

Extended Data Figure 8, Camargo Ortega et al.

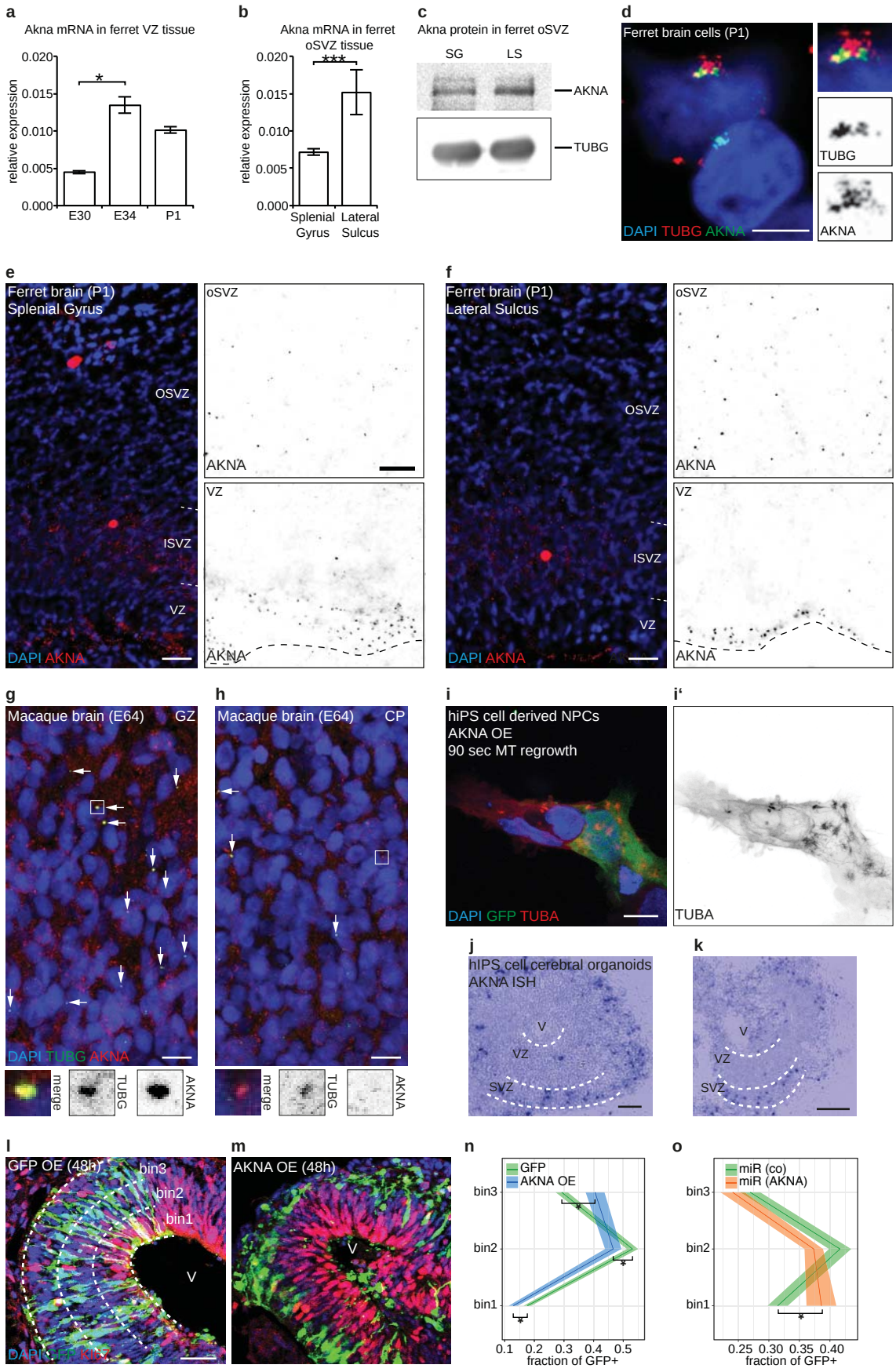

Extended Data Figure 9, Camargo Ortega et al.,

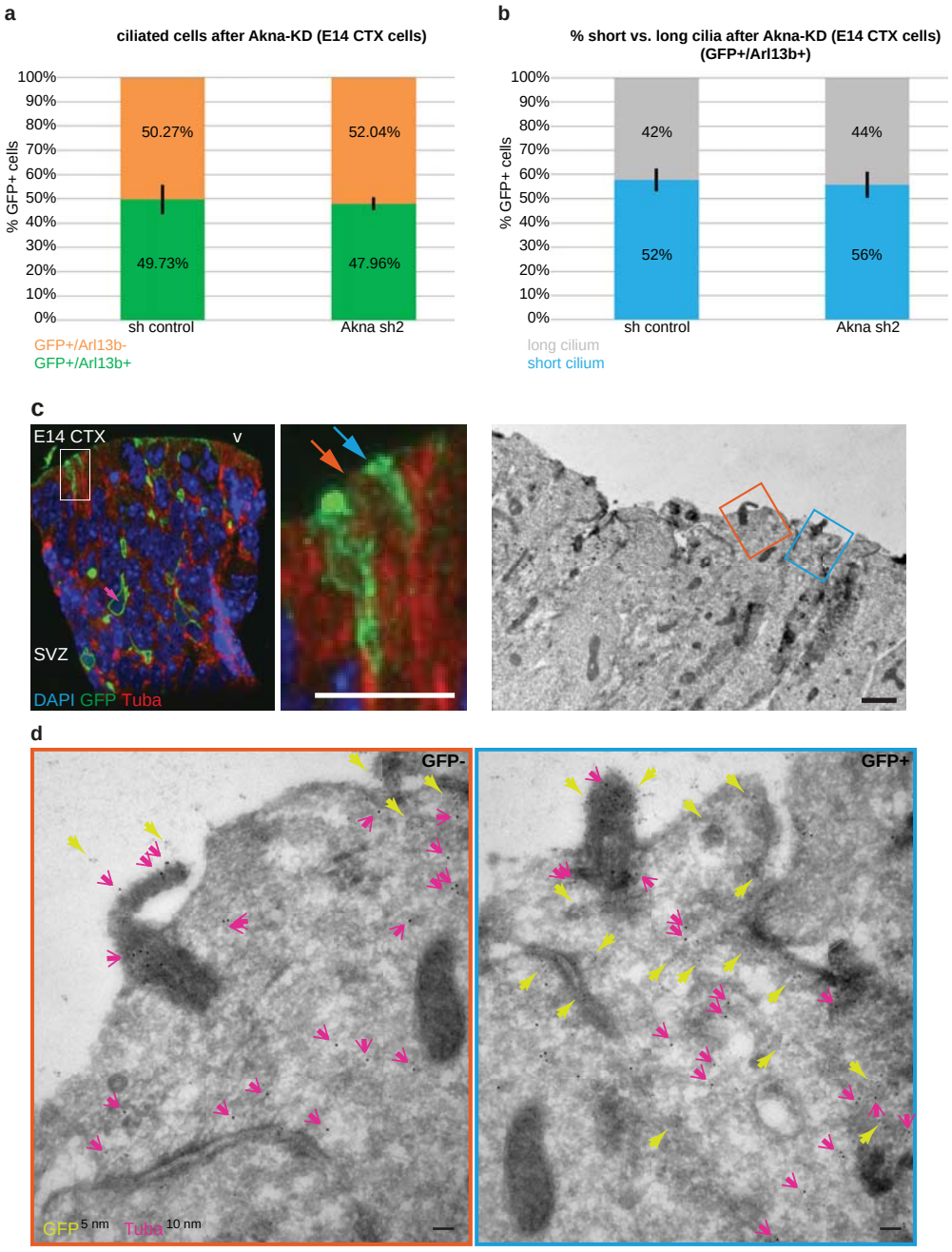

Extended Data Figure 10 Camargo Ortega et al.